

Non-linear X-ray optics (FWM) with FELs

C. Masciovecchio

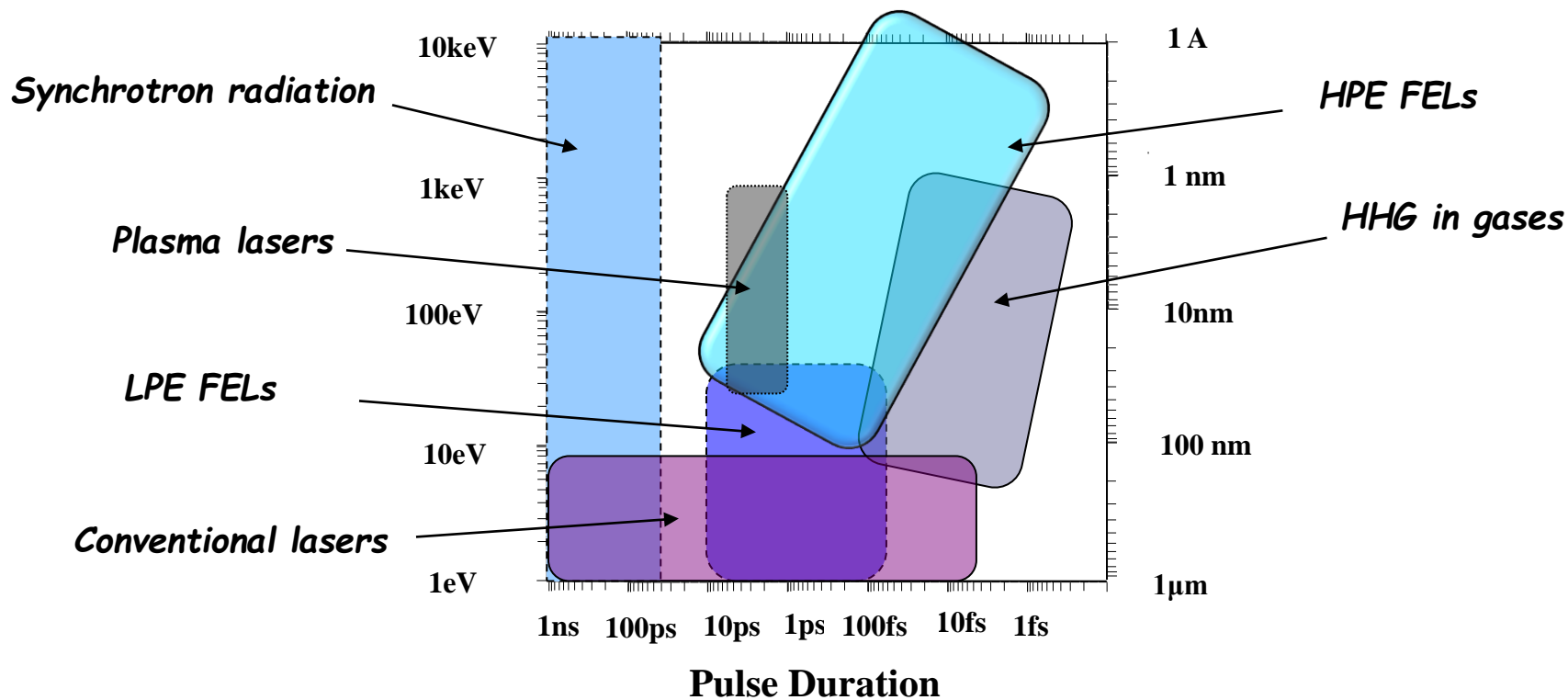
Elettra – Sincrotrone Trieste



Elettra Sincrotrone Trieste



Why Free Electron Lasers ?



Imaging with high Spatial Resolution ($\sim \lambda$): fixed target imaging, particle injection imaging,...

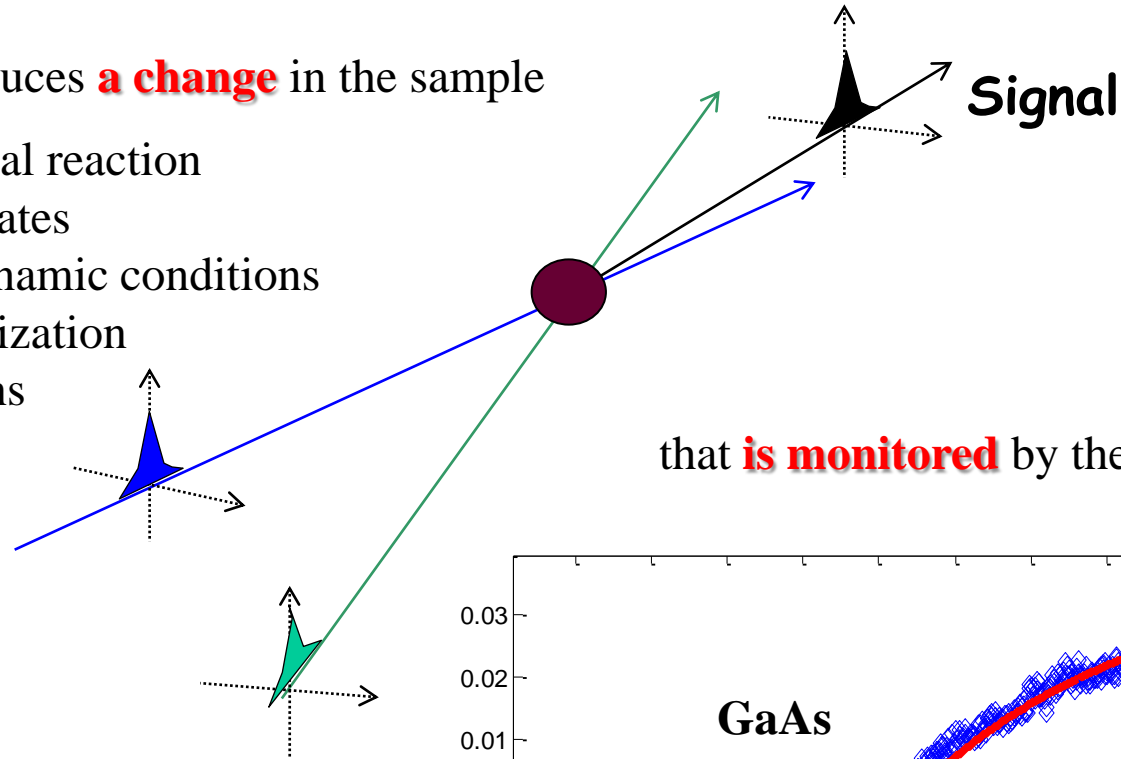
Dynamics: wave mixing (nanoscale), warm dense matter, extreme condition,

Resonant Experiments: XANES (tunability), XMCD (polarization), chemical mapping,

Pump & Probe

The **pump** pulse produces **a change** in the sample

- stimulate a chemical reaction
- non-equilibrium states
- extreme thermodynamic conditions
- ultrafast demagnetization
- coherent excitations
-

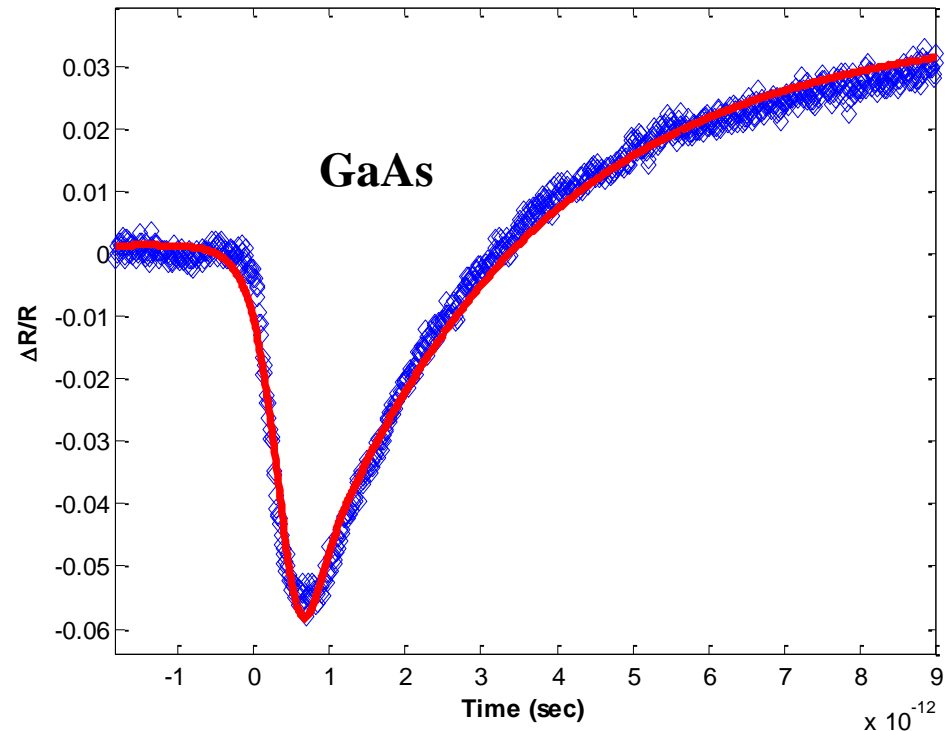


that **is monitored** by the **probe** pulse

WORLD RECORD !!

Jitter ~ 5 fs

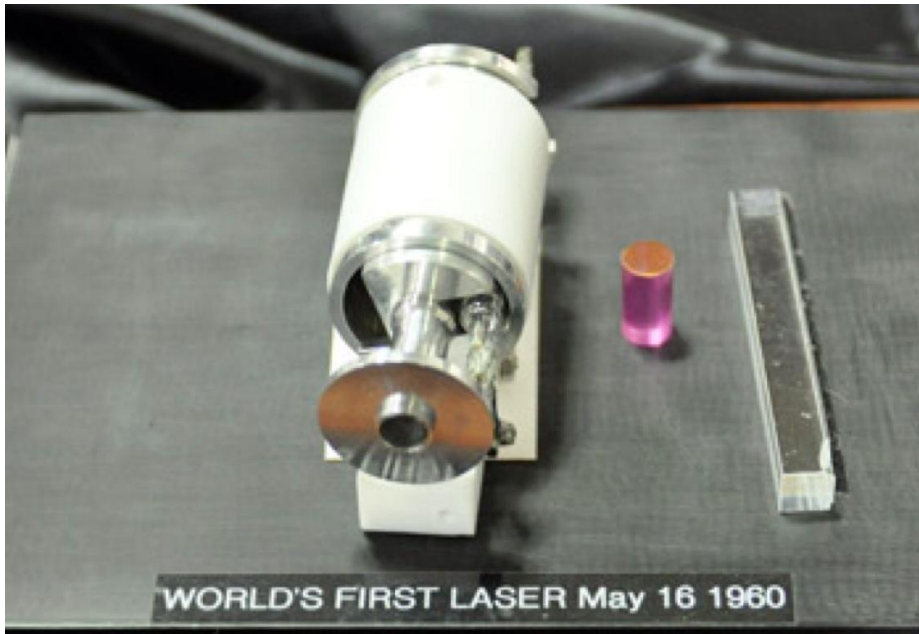
M. Danailov et al., Opt. Exp. (2014)



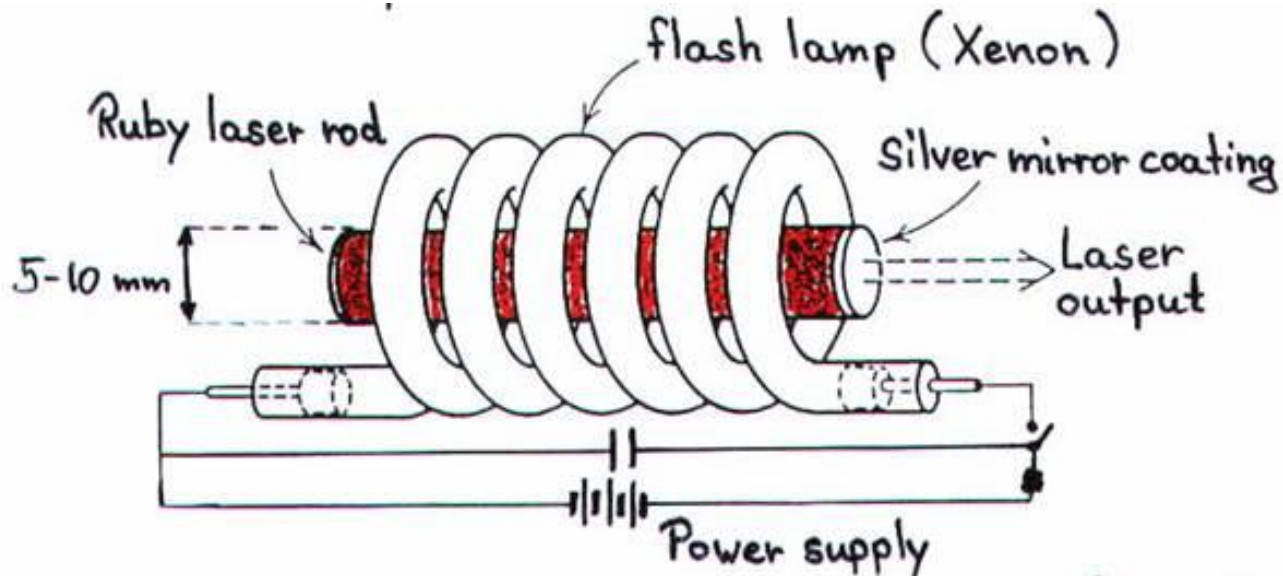
The Advent of Lasers



Elettra Sincrotrone Trieste



T. H. Maiman
Recognized Stanford Engineering Hero



- **1964**: A. M. Prokhorov, C. H. Townes & N. G. Basov → fundamental work in **theory**
- **1971**: D. Gabor → theory of **holography** in the late 1940's developed thanks to the laser advent
- **1981**: N. Bloembergen & A L. Schawlow → laser spectroscopy and **non-linear** optical effects
- **1989**: N. F. Ramsey → hydrogen maser
- **1997**: S. Chu, C. Cohen-Tannoudji & William D. Phillips → laser cooling
- **2001**: E. A. Cornell, W. Ketterle & C. E. Wieman → laser cooling (Bose-Einstein condensation)
- **2005**: J. L. Hall & T. W. Hänsch → optical **frequency comb** technique
- **2006**: J. C. Mather & G. F. Smoot → measure the cosmic microwave background radiation
- **2009**: C. K. Kao → development of **fiber optics** in telecommunications
- **1999**: A. Zewail → femtosecond spectroscopy (**femtochemistry**) to picture chemical reactions
- **20XX X. Xxx** → **Free Electron Laser ?**



N. Bloembergen 1981



Non linear techniques are powerful experimental tools when one wants

- 1) to measure **sample properties** that cannot be addressed by *conventional* linear optical spectroscopy or
- 2) to obtain spectroscopic information with a higher **resolution** or **sensitivity** than that associated with linear spectroscopy

GENERATION OF OPTICAL HARMONICS*

P. A. Franken, A. E. Hill, C. W. Peters, and G. Weinreich

The Harrison M. Randall Laboratory of Physics, The University of Michigan, Ann Arbor, Michigan

(Received July 21, 1961)



FIG. 1. A direct reproduction of the first plate in which there was an indication of second harmonic. The wavelength scale is in units of 100 Å. The arrow at 3472 Å indicates the small but dense image produced by the second harmonic. The image of the primary beam at 6943 Å is very large due to halation.



Famously, when published in the journal *Physical Review Letters*, the copy editor mistook the dim spot (at 347 nm) on the photographic paper as a **speck of dirt** and removed it from the publication.

Polarization and Susceptibility

$$\mathbf{P}(\omega) = \chi(\omega) \cdot \mathbf{E}(\omega)$$

When the electric field of the light is intense, χ itself **depends on the electric field** and thus the polarization can be expressed in a power series of E

$$\mathbf{P} = \mathbf{P}^L + \mathbf{P}^{NL} = \varepsilon_0 \left[\chi^{(1)} \cdot \mathbf{E} + \chi^{(2)} \cdot \mathbf{E} \cdot \mathbf{E} + \chi^{(3)} \cdot \mathbf{E} \cdot \mathbf{E} \cdot \mathbf{E} \right]$$

\swarrow \swarrow \swarrow

≈ 1 $\approx 10^{-12} \text{ m/V}$ $\approx 10^{-23} \text{ m}^2/\text{V}^2$

The **atomic field** is $E_a \approx 0.5 \cdot 10^{12} \text{ V/m}$

$I \text{ (W/cm}^2\text{)}$

$E_0 \text{ (V/m)}$

$$10^{15} \text{ (100 fs, } 10 \text{ } \mu\text{J, } 10 \mu\text{m)} \rightarrow 10^{12}$$

Second Order Non-linear Susceptibility



Elettra Sincrotrone Trieste

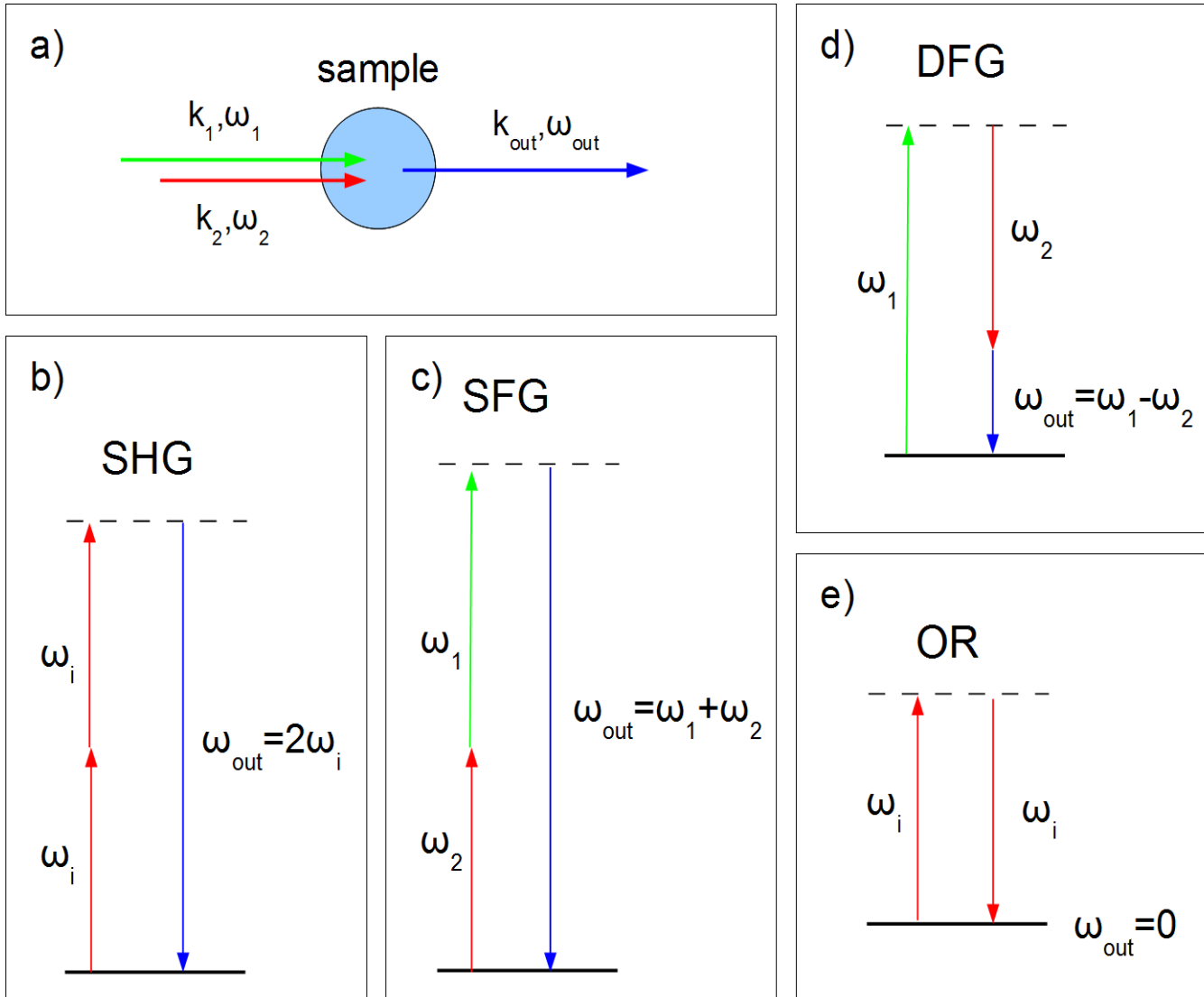
$$P = \varepsilon_0 \cdot \left[\left(\sum_i \chi^{(1)} \cdot E_i \right) + \left(\sum_{ij} \chi^{(2)} \cdot E_i \cdot E_j \right) + \left(\sum_{ij,k} \chi^{(3)} \cdot E_i \cdot E_j \cdot E_k \right) + \dots \right]$$
$$= P^{(1)} + P^{(2)} + P^{(3)} + \dots = P^{(L)} + P^{(NL)},$$

$$\frac{P^{(2)}}{\varepsilon_0} = [\chi^{(2)}(2 \cdot \omega_1) \cdot E_1'^2 \cdot \exp(-2 \cdot i \cdot \omega_1 \cdot t) + \chi^{(2)}(2 \cdot \omega_2) \cdot E_2'^2 \cdot \exp(-2 \cdot i \cdot \omega_2 \cdot t)$$
$$+ 2 \cdot \chi^{(2)}(\omega_1 + \omega_2) \cdot E_1' \cdot E_2' \cdot \exp(-i \cdot (\omega_1 + \omega_2) \cdot t)$$
$$+ 2 \cdot \chi^{(2)}(\omega_1 - \omega_2) \cdot E_1' \cdot E_2' \cdot \exp(-i \cdot (\omega_1 - \omega_2) \cdot t) + C.C.]$$
$$+ 2 \cdot \chi^{(2)}(\omega = 0) \cdot [E_1' \cdot E_2'^* + E_1'^* \cdot E_2']$$

Second Order Processes



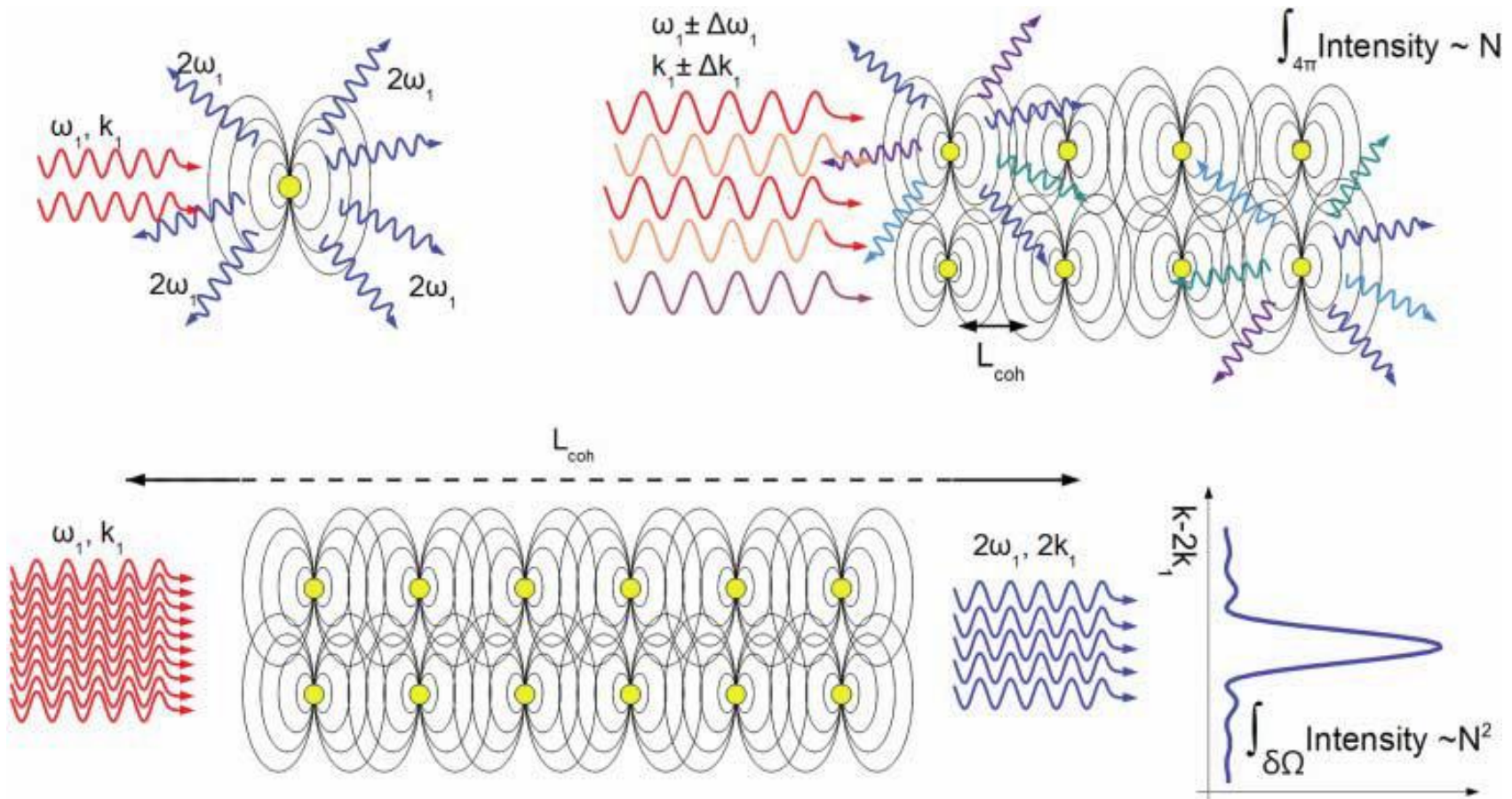
Elettra Sincrotrone Trieste

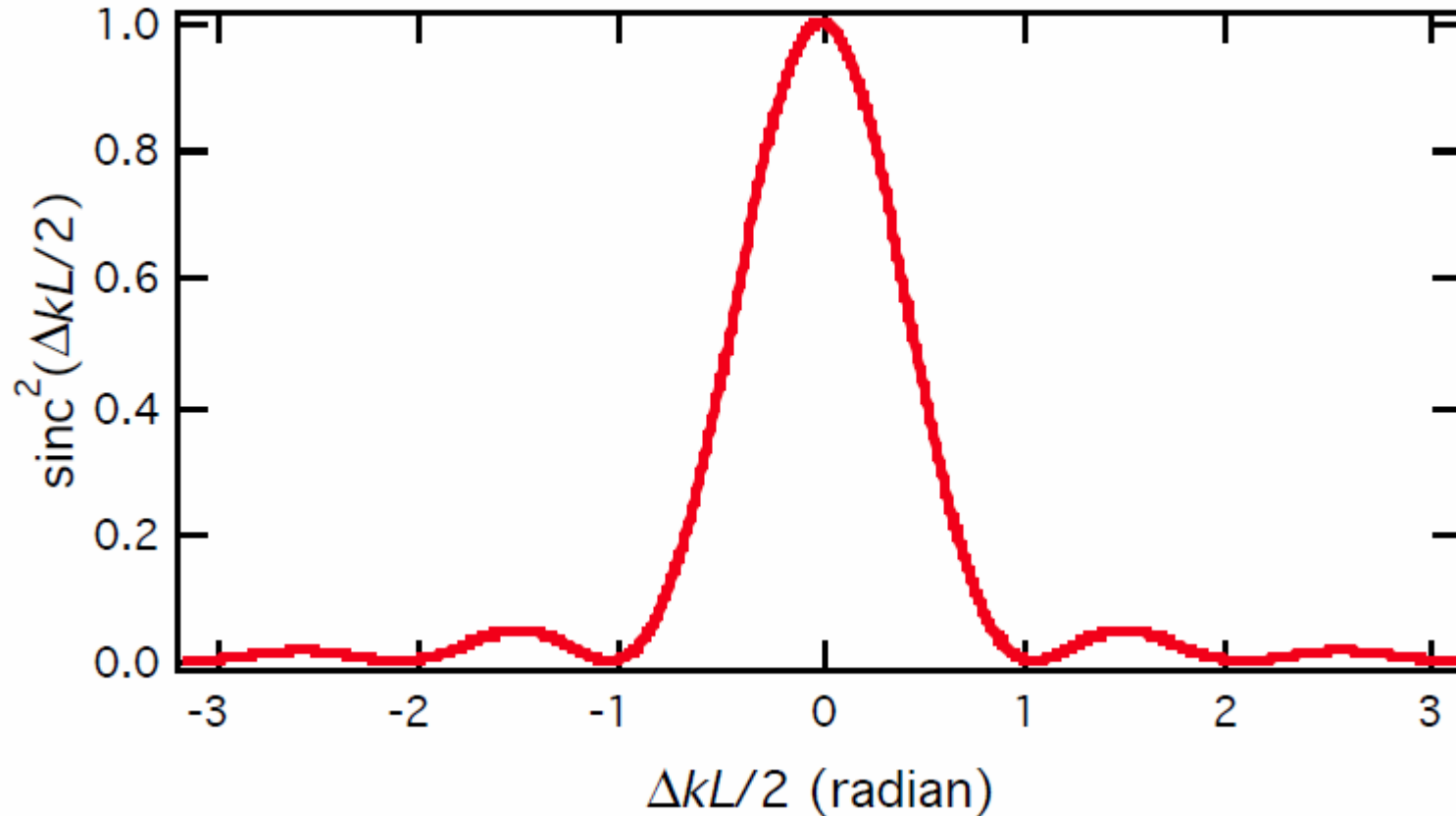


Second Order Processes



Elettra Sincrotrone Trieste





$$I_i(\omega_3) \propto |\chi_{ijk}^{(2)}|^2 I_j I_k L^2 \cdot \text{sinc}^2\left(\frac{\Delta k L}{2}\right)$$

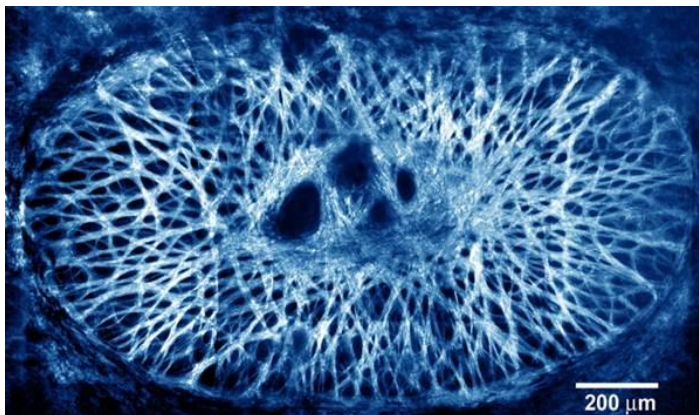
$$\Delta k = \mathbf{k}_{out} - \sum \mathbf{k}_{in}$$

Media with inversion symmetry are forbidden from generating second harmonic light

$$\mathbf{P} = \mathbf{P}^L + \mathbf{P}^{NL} = \varepsilon_0 \left[\chi^{(1)} \cdot \mathbf{E} + \chi^{(2)} \cdot \mathbf{E} \cdot \mathbf{E} + \chi^{(3)} \cdot \mathbf{E} \cdot \mathbf{E} \cdot \mathbf{E} \right]$$

surfaces and interfaces make interesting subjects for study with SHG and SFG

In fact, second harmonic generation and sum frequency generation discriminate against signals from the bulk, implicitly labeling them as surface specific techniques.

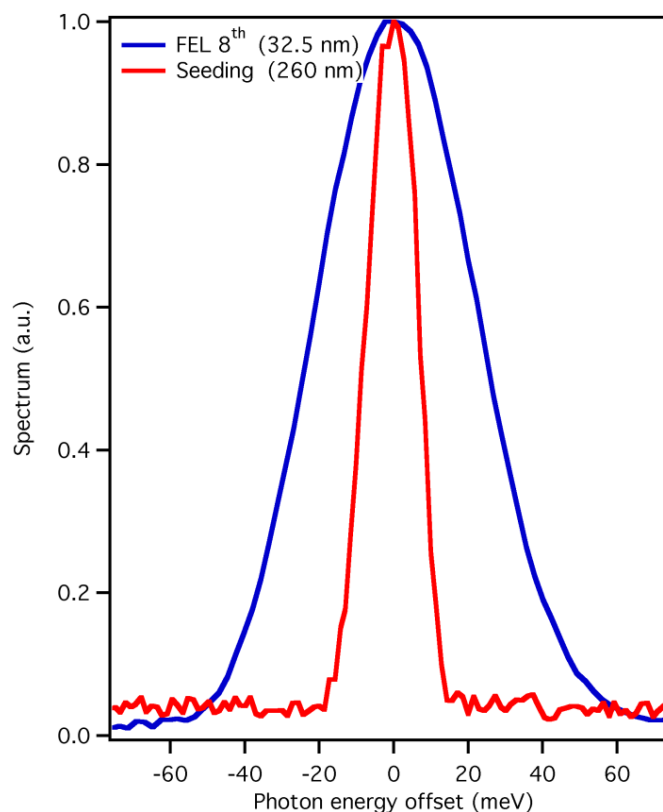
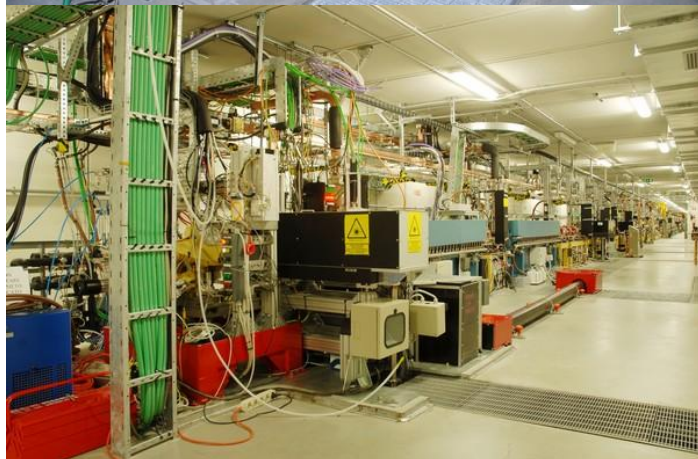


Imaging of lamina cribrosa collagen structure
in the optic nerve of the eye

Reduced photo-toxicity →
→ **biological imaging**

Highly coherent and stable pulses from the FERMI seeded free-electron laser in the extreme ultraviolet

E. Allaria et al (2012)



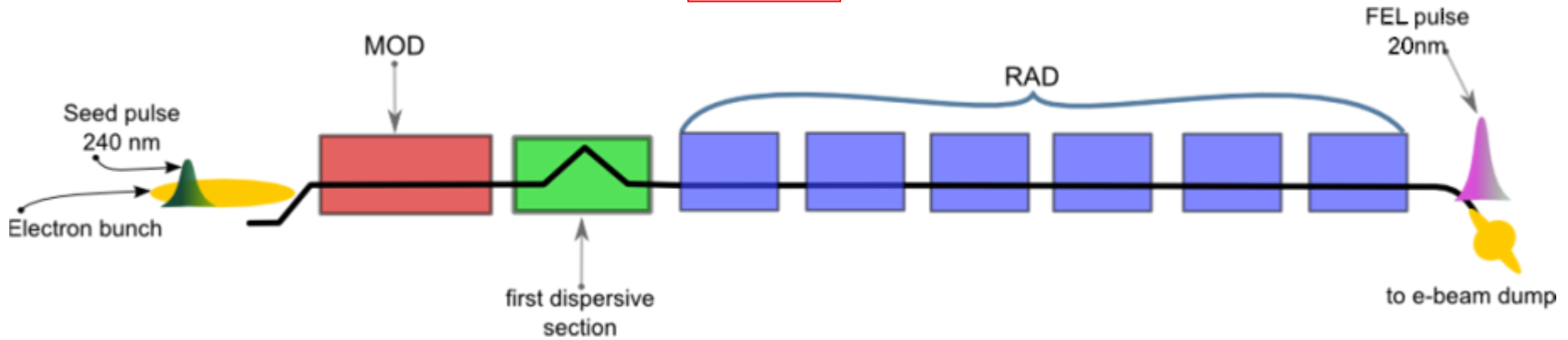
$\Delta t < 100$ fs
Flux $< 10^{14}$ ph/pulse
 $E \sim 20 - 800$ eV
Total Control on
Pulse Energy
Time Shape
Polarization

FEL1 and FEL2



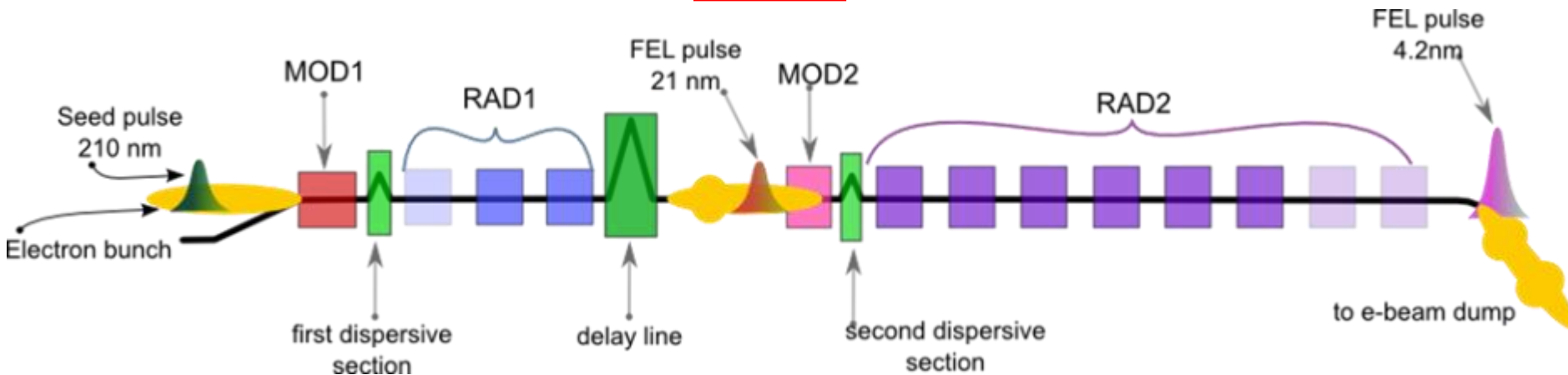
Elettra Sincrotrone Trieste

FEL 1



E. Allaria et al., Nat. Phot. (2012)

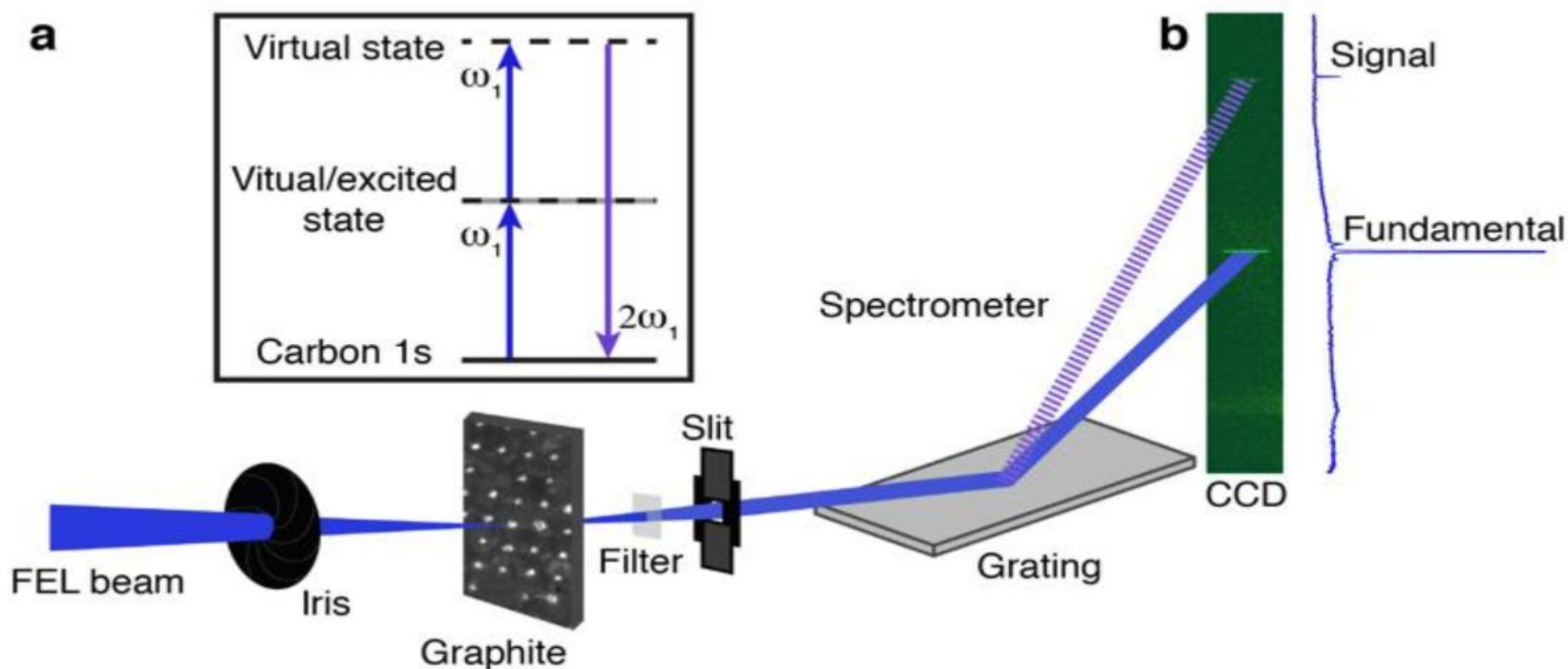
FEL 2



E. Allaria et al., Nat. Phot. (2014)

Second Harmonic Generation @ FERMI

$$P_i = \chi_{ij}^{(1)} E_j + \chi_{ijk}^{(2)} E_j E_k + \chi_{ijkl}^{(3)} E_j E_k E_l + \dots$$

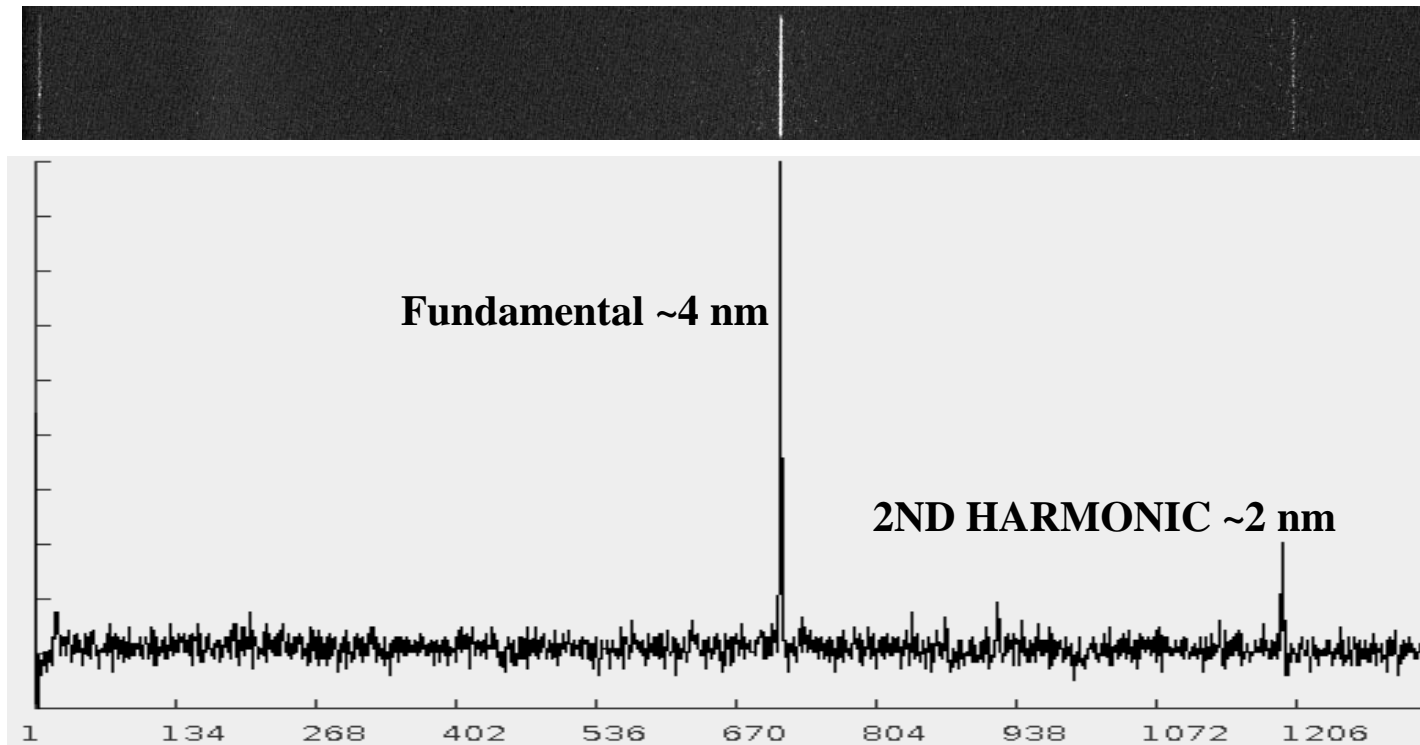


R. Lam et al., PRL (2018)

Second Harmonic Generation @ FERMI

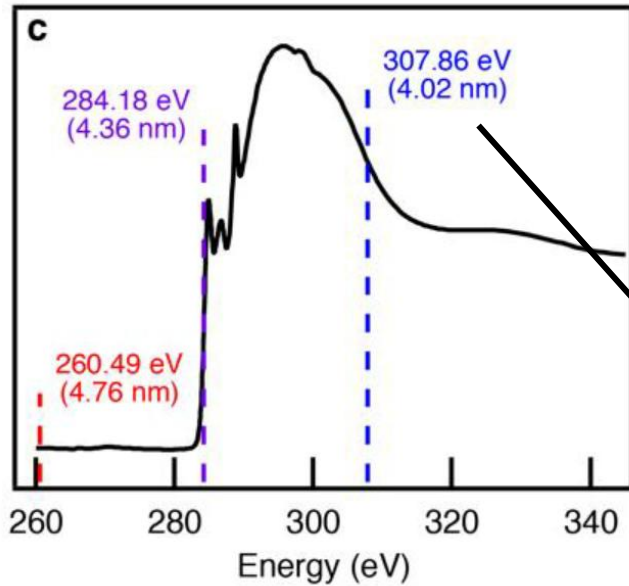
2nd harmonic generation from graphite

FEL primary beam at about 4 nm (**C K-edge**)



Spectrum from graphite in transmission geometry from **single shot**

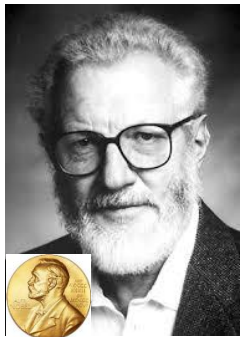
Second Harmonic Generation @ FERMI



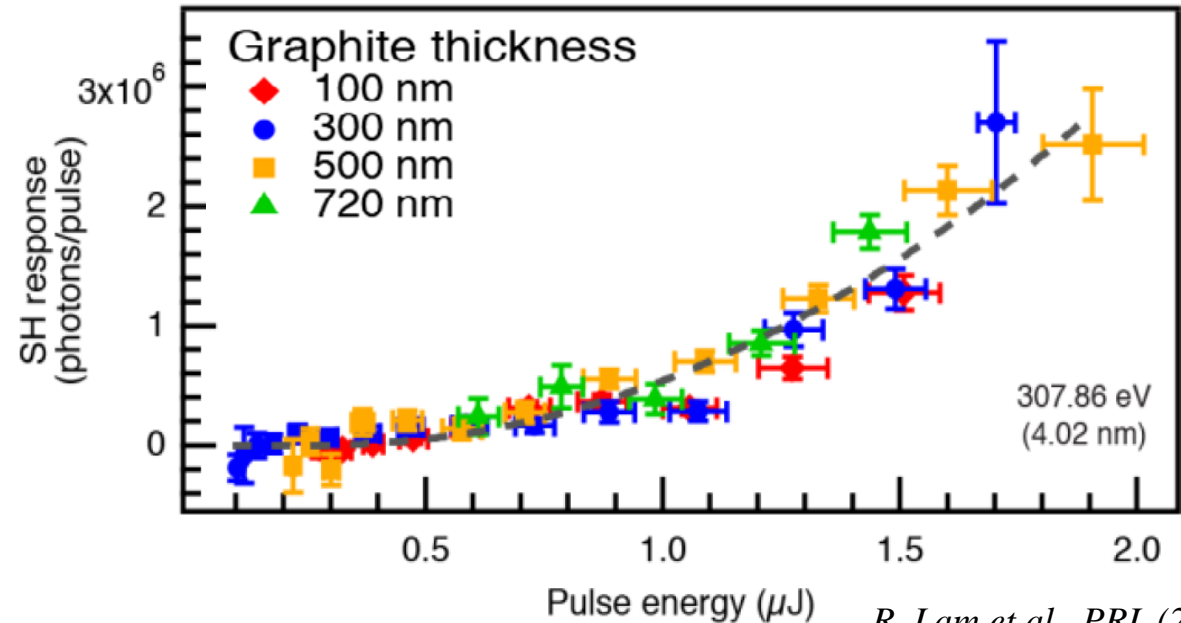
NO thickness dependence of SHG signal



Measure local geometric and/or electronic structure of a **single atomic layer**



H. Kroemer 2000



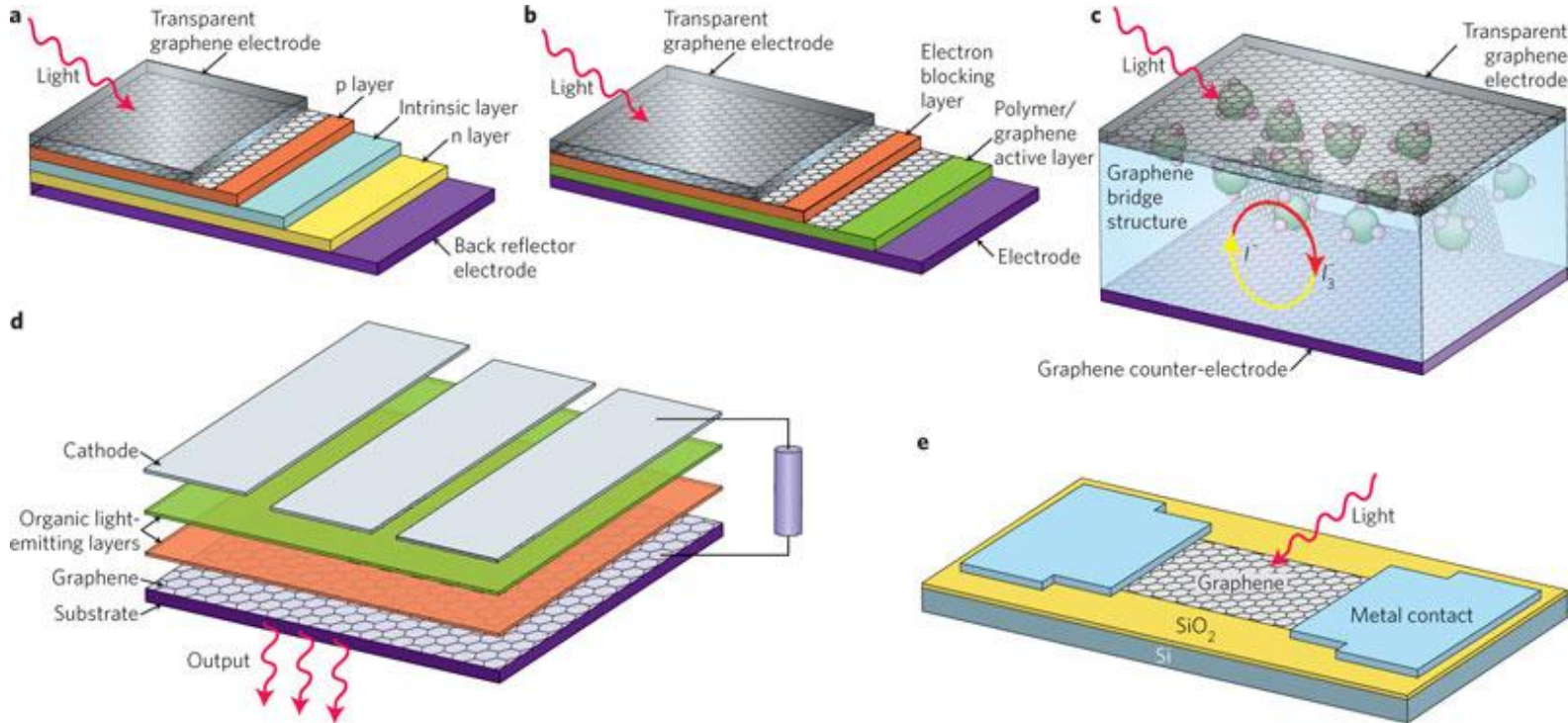
R. Lam et al., PRL (2018)

The interface is the device!

Second Order Processes at shorter λ



Elettra Sincrotrone Trieste



→ New class of surface analysis

- Significantly **higher surface specificity** than existing soft X-ray methods
- Study of **catalytic interfaces**, electrode surfaces, **photovoltaics**, microelectronics

As the surfaces and interfacial properties of materials are known to significantly affect their performance, understanding these properties is essential to improvements

X-Ray Probe Targets Interfaces

A new spectroscopy technique employs x rays from a free electron laser to probe the properties of interfaces that may be hidden within a material.

by Anders Nilsson*

Interfaces are what separate one material from another. We sense the world through interfaces, whether touching the surface of a table or seeing the light reflecting off the edge of a glass. Many other interfaces are less visible but still have a place in our lives. Modern solar cells consist of thin layers where interfaces play an important role for charge separation. Catalytic reactions for chemical energy transformations occur at solid-gas or solid-liquid interfaces. It is extremely challenging to probe these interfaces, as they are often buried under layers or in contact with a liquid or high-pressure gas where the number of interface atoms is extremely small in comparison to the surrounding material [1]. Researchers, therefore, search for techniques that are only sensitive to the two-dimensional interface. Royce Lam from the University of California, Berkeley, and colleagues have developed an interfacial probe utilizing soft-x-ray pulses from a free electron laser [2]. By aiming the pulses at a graphite sample, the scientists have shown that they can detect a nonlinear spectrographic signal that arises from the graphene layers near the surface of the graphite. This demonstration opens up a new field in interface studies, offering the possibility to track surface chemistry reactions with the femtosecond resolution provided by the very short x-ray pulses from free electron lasers.



SPECTROSCOPY

► Soft X-rays probe buried interfaces

Second-harmonic generation (SHG) is a nonlinear optical process in which two photons of a given energy interact with select types of materials and combine to form a single photon with double the original energy. The SHG process, and a closely related one known as sum frequency generation, lie at the heart of a number of spectroscopy methods based on infrared, visible, and ultraviolet laser light. As a result of spectroscopy selection rules, these nonlinear processes are particularly adept at probing interfaces, even ones hidden by many layers of molecules, as is the case for a solid catalyst in contact with high-pressure gas or an electrode in contact with a liquid-electrolyte solution. X-rays with photons in the 100-to-1,000-eV energy range, so-called soft X-rays, can provide valuable information about chemical bonding and structure with elemental specificity. But because of the lack of available light sources with the required intensity and coherence, researchers have been unable to develop an SHG version of soft X-ray interface spectroscopy—until now. In a proof-of-concept study, Richard J. Saykally and a large team of researchers working at the FERMI facility in Trieste, Italy, have demonstrated that the method can selectively probe layers of graphene inside a graphite sample (*Phys. Rev. Lett.* 2018, DOI: 10.1103/physrevlett.120.023901). The new technique may eventually enable researchers to use X-rays to track chemical reactions at interfaces with femtosecond



C&E News (ACS)



N. Bloembergen 1981



$$P_i = \chi_{ij}^{(1)} E_j + \chi_{ijk}^{(2)} E_j E_k + \chi_{ijkl}^{(3)} E_j E_k E_l + \dots$$

Is **zero** for media with inversion symmetry

is the lowest nonlinear order for centrosymmetric materials →
→ **all materials** have a third-order nonlinear response

FOUR-WAVE MIXING SPECTROSCOPY

The nonlinearity $\chi^{(3)}$ describes a coupling between four light waves, and some typical wave-vector geometries which satisfy both energy and momentum conservation of the electromagnetic fields *N. Bloembergen Nobel Lecture 1981*

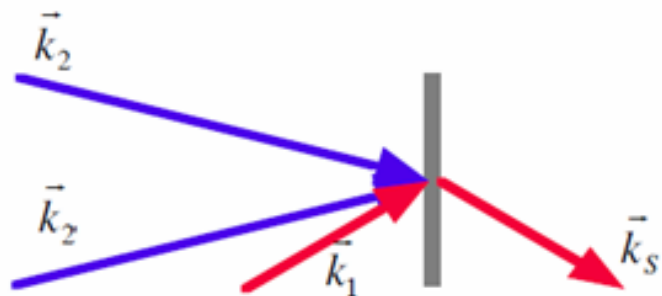
$$\omega_1 + \omega_2 + \omega_3$$

$$3\omega_j, \omega_j \quad j=1,2,3$$

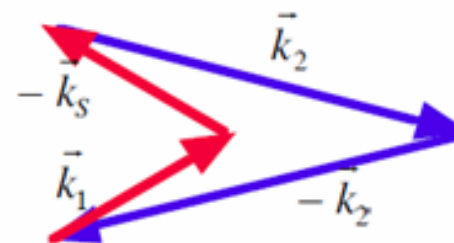
$$2\omega_i + \omega_j, 2\omega_i - \omega_j, \omega_i - 2\omega_j$$

$$\omega_i + \omega_j - \omega_k, \omega_i - \omega_j - \omega_k$$

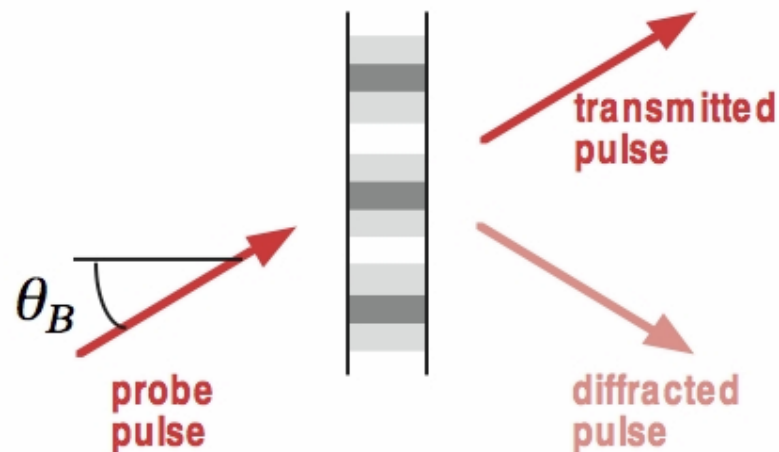
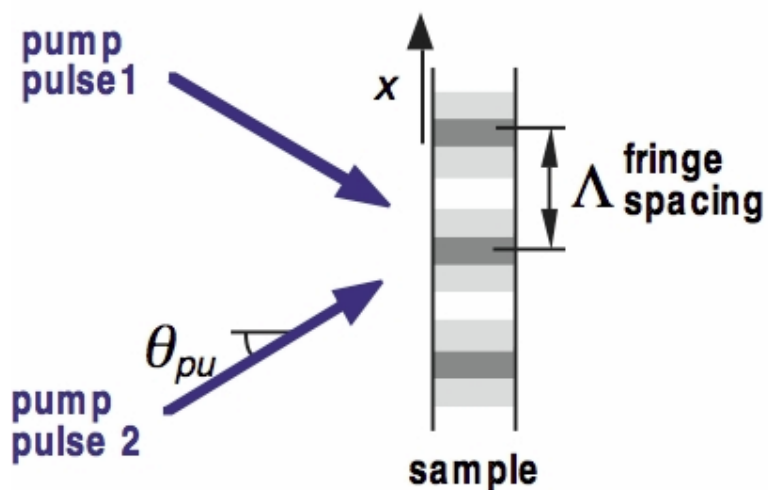
Transient Grating



$$\omega_s = \omega_1 + \omega_2 - \omega_2$$

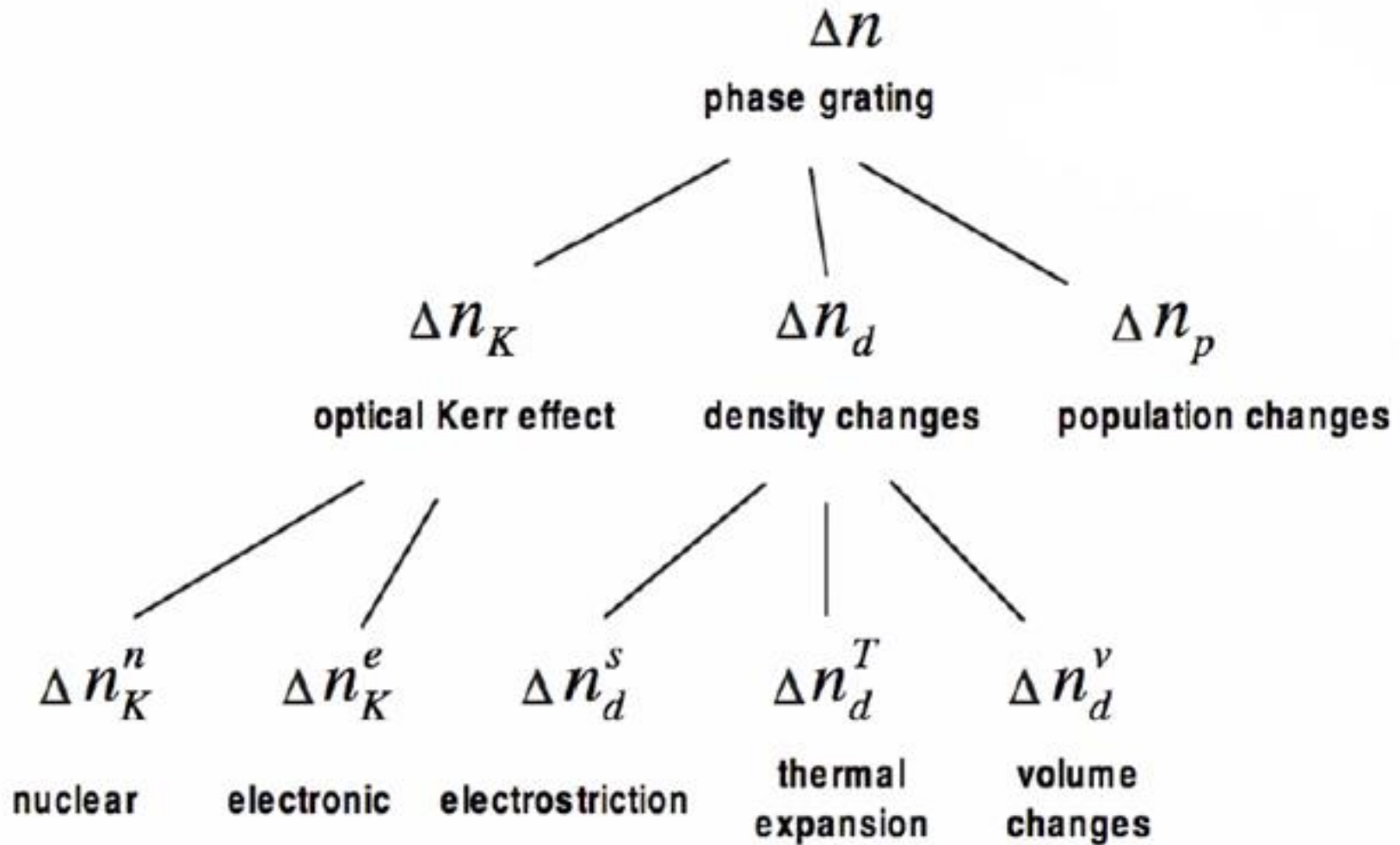


$$\Delta \vec{k} = \vec{k}_1 + \vec{k}_2 - \vec{k}_2 - \vec{k}_s = 0$$



The phase matching ensures the **signal cleanness**

Refractive Index Changes



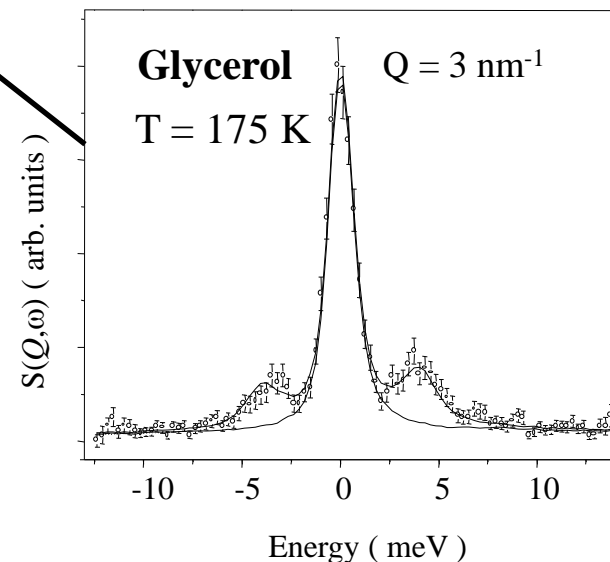
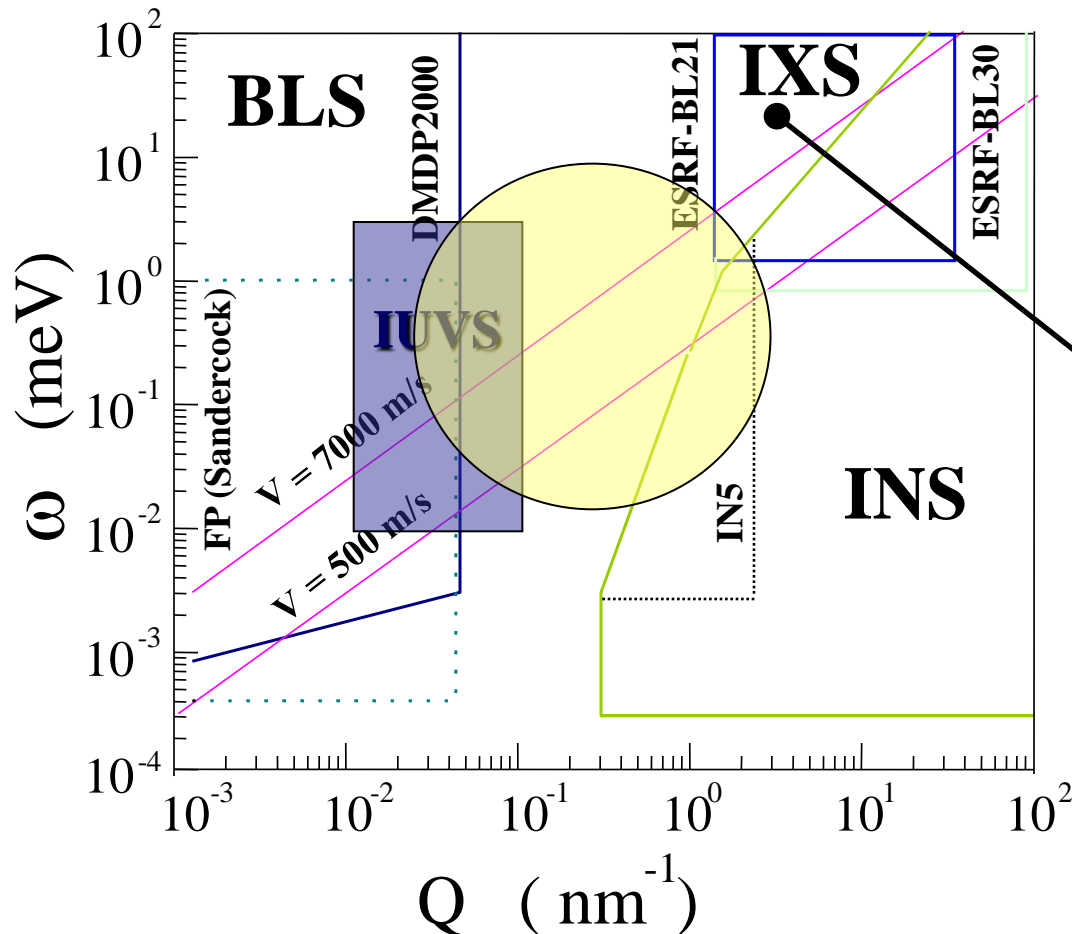
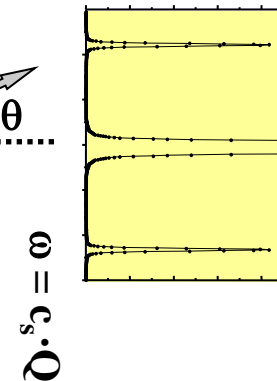
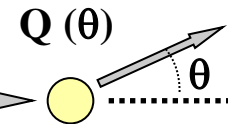
Collective Dynamics at the Nanoscale



Elettra Sincrotrone Trieste

Challenge: Study Collective Excitations in **Disordered Systems**
in the **Unexplored** ω - Q region

Determination of the Dynamic Structure Factor: $S(Q, \omega)$



Why Disordered Systems ?



Elettra Sincrotrone Trieste

UNSOLVED PROBLEMS IN PHYSICS



Condensed matter physics

Amorphous solids

What is the nature of the [transition](#) between a fluid or regular solid and a glassy [phase](#)? What are the physical processes giving rise to the general properties of glasses?

High-temperature superconductors

What is the responsible mechanism that causes certain materials to exhibit [superconductivity](#) at temperatures much higher than around 50 [Kelvin](#)?

Sonoluminescence

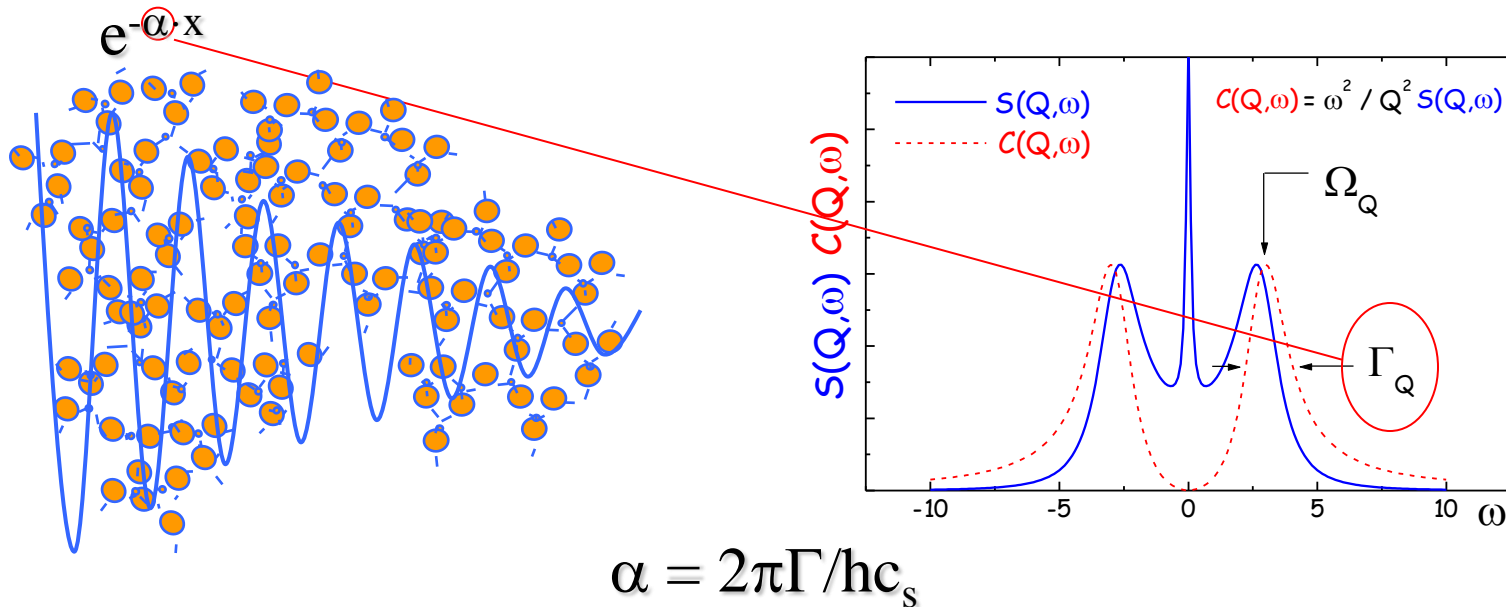
What causes the emission of short bursts of light from imploding bubbles in a liquid when excited by sound?

Turbulence

Is it possible to make a theoretical model to describe the statistics of a turbulent flow (in particular, its internal structures)? Also, under what conditions do [smooth solution to the Navier-Stokes equations](#) exist?

Glass is a **very general state** of condensed matter → a large variety of systems can be transformed from liquid to glass

The liquid-glass transition cannot be described in the framework of classical phase transitions since T_g depends on the **quenching rate** → one cannot define an **order parameter** showing a critical behaviour at T_g



Sound Attenuation in Glasses is very different from their Crystalline Counterpart



Understanding of **Thermal Anomalies** (Specific Heat and Thermal Conductivity)

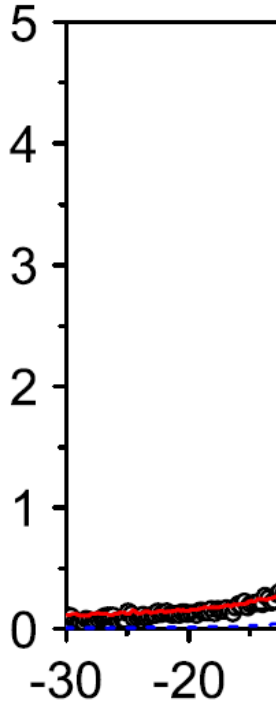
At low Q 's Γ exhibit a Q^2 dependence at (and above) room temperature which **does not extrapolate** to the Q^2 measured by IXS

Why at the nanoscale ?

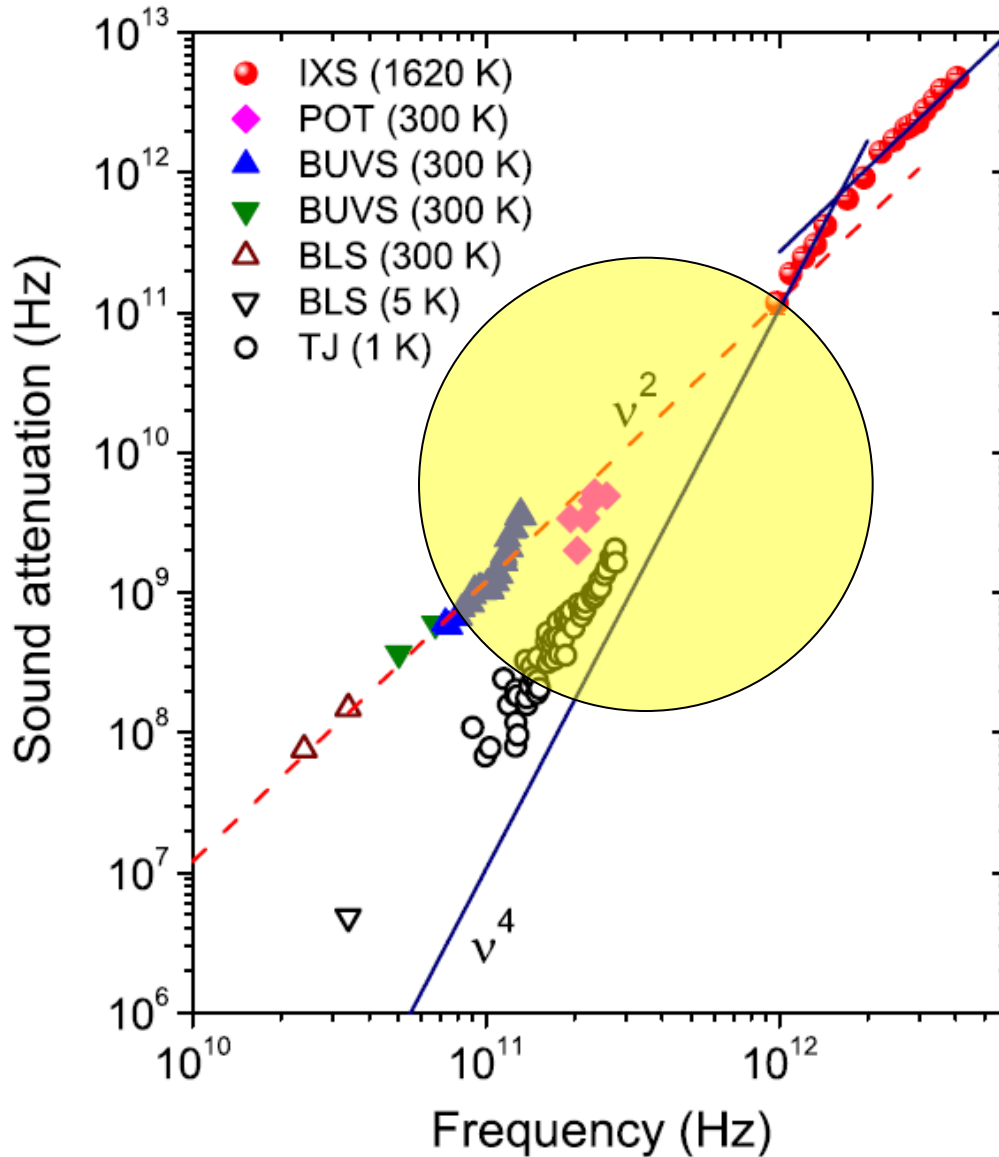


Elettra Sincrotrone Trieste

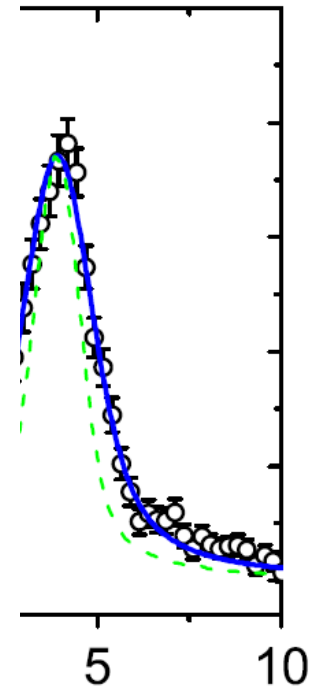
The nature of



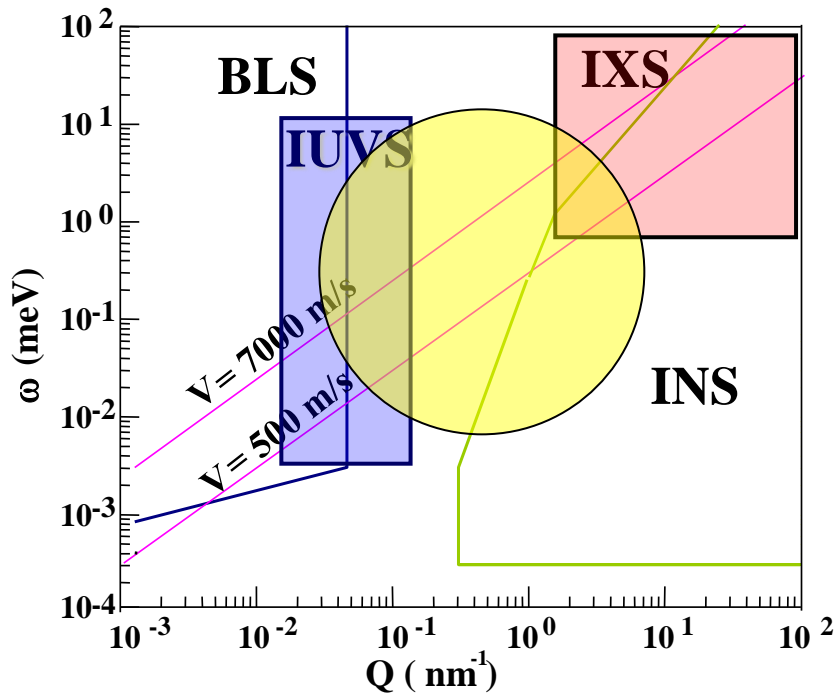
Func



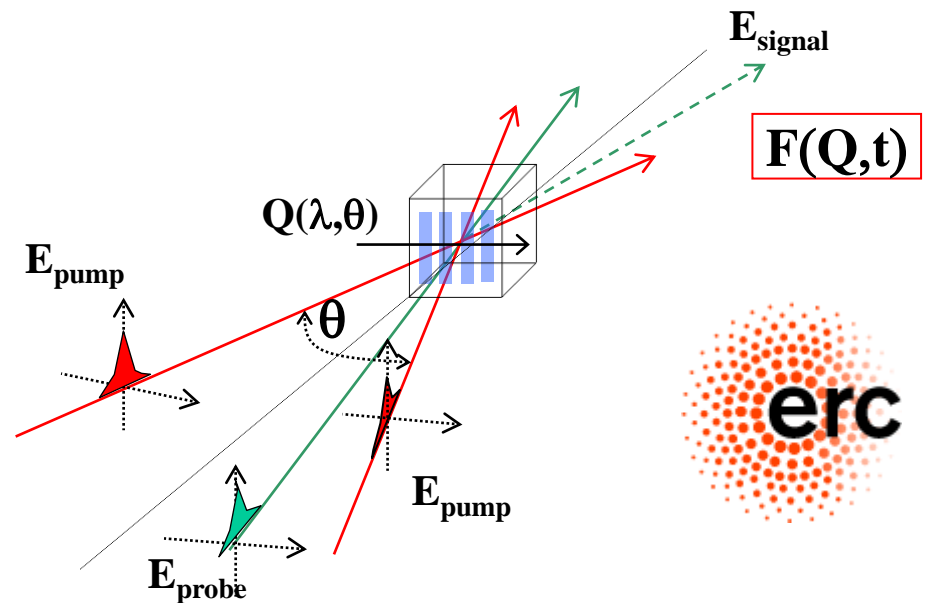
ar (V-SiO₂)



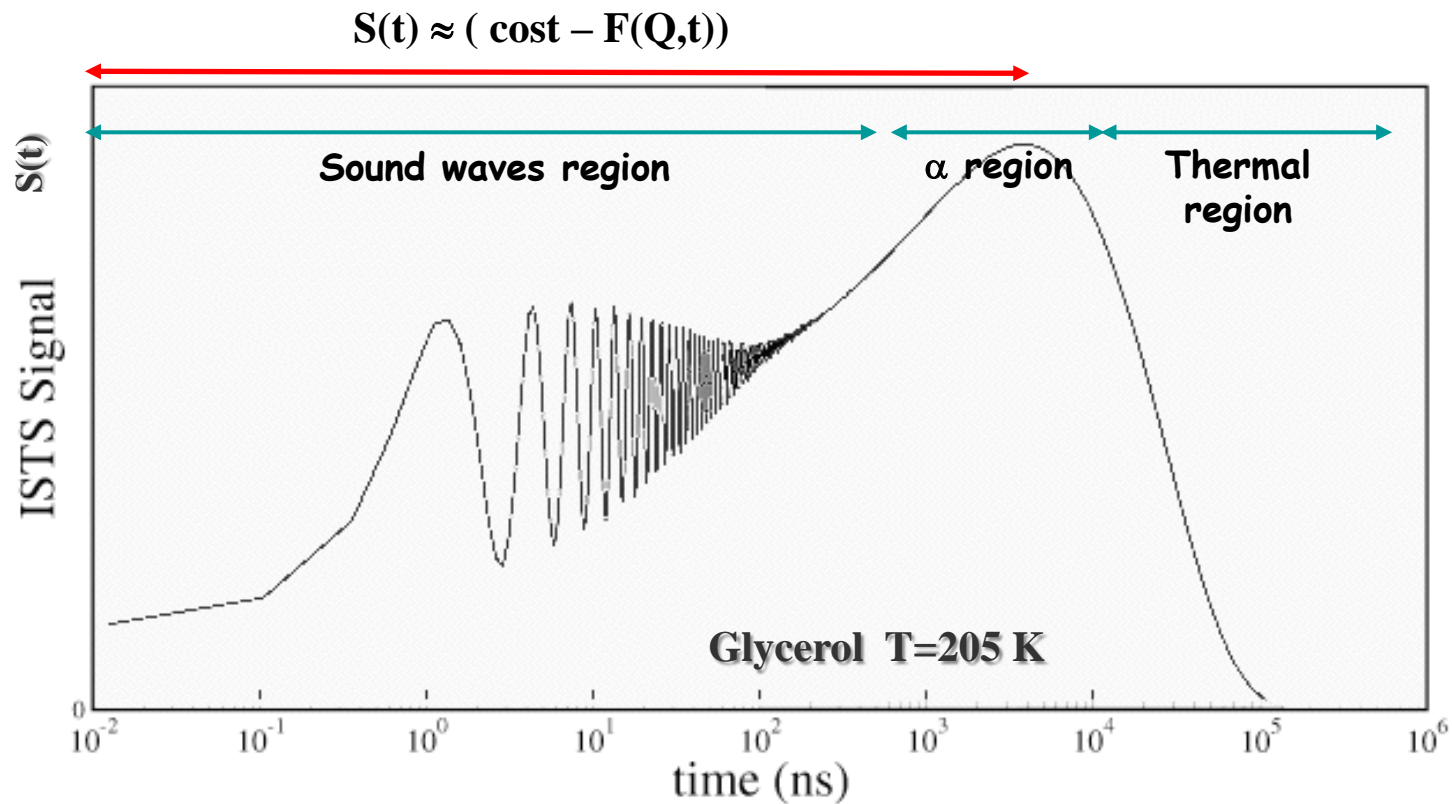
S



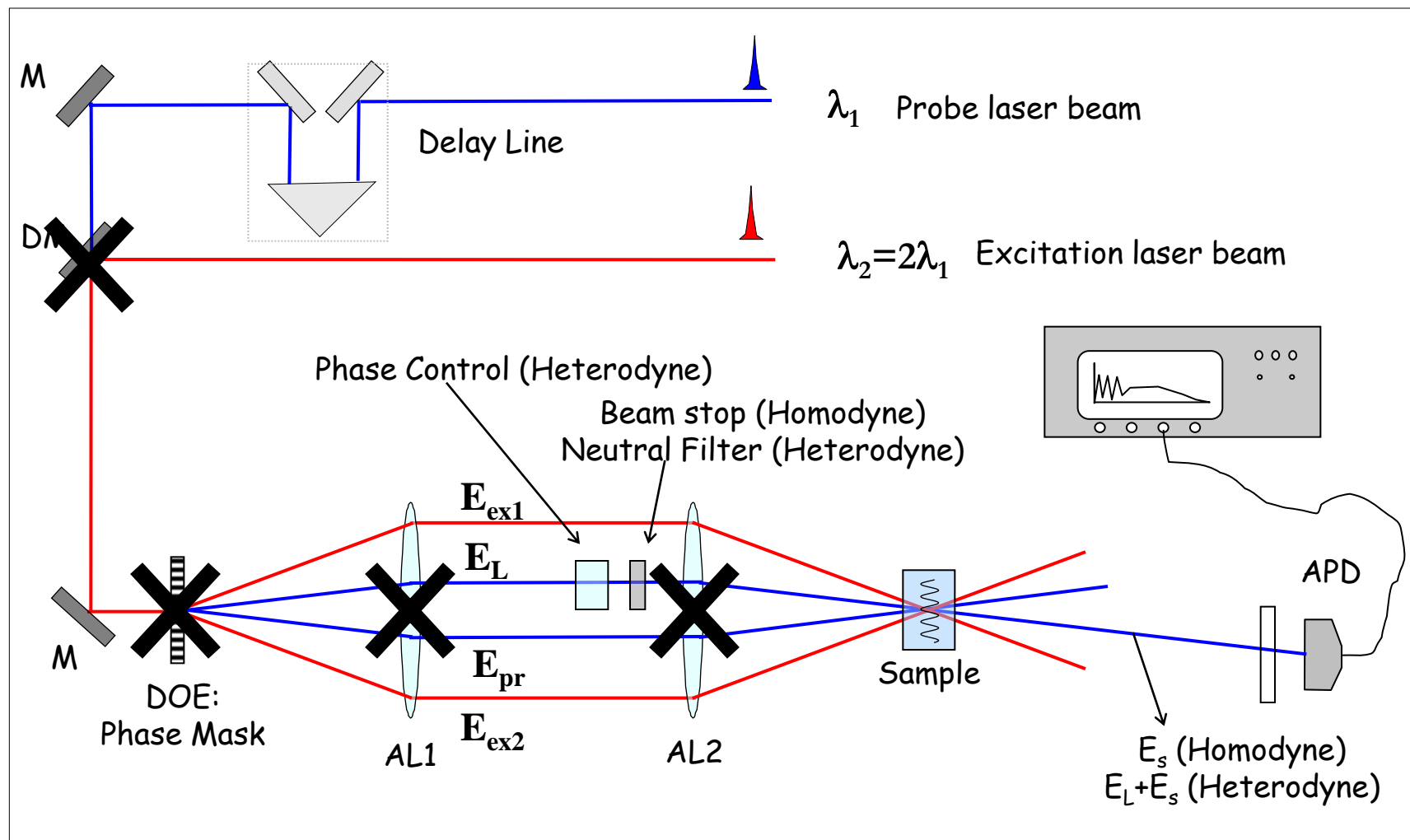
Solution: Free Electron Laser based Transient Grating Spectroscopy



Optical absorption \rightarrow Temperature Grating \rightarrow Time-dependent Density Response
(driven by thermal expansion)

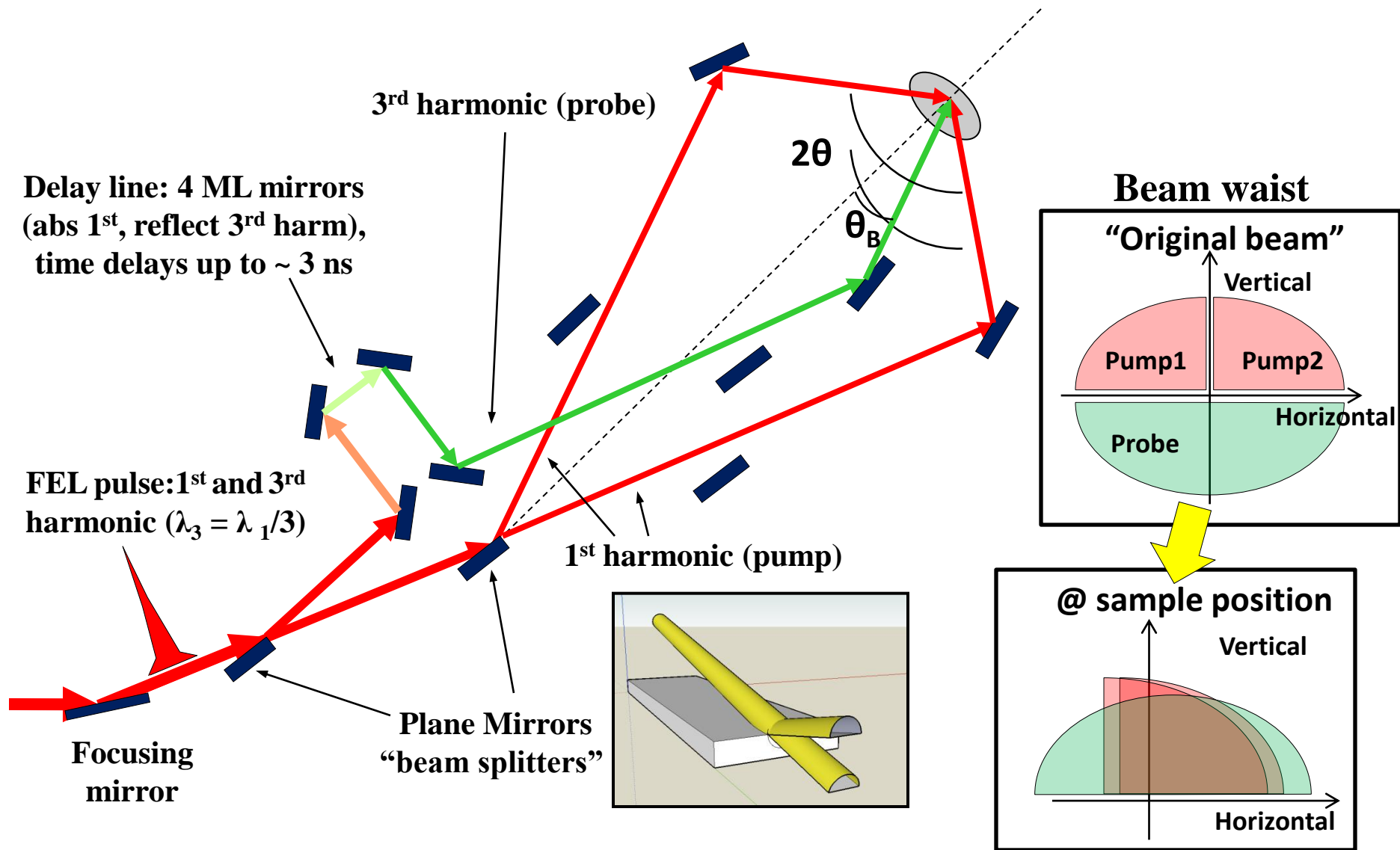


Typical Infrared/Visible Set-Up



Challenge: Extend and modify the set-up for UV Transient Grating Experiments

Beam parameters



Expected TG formation

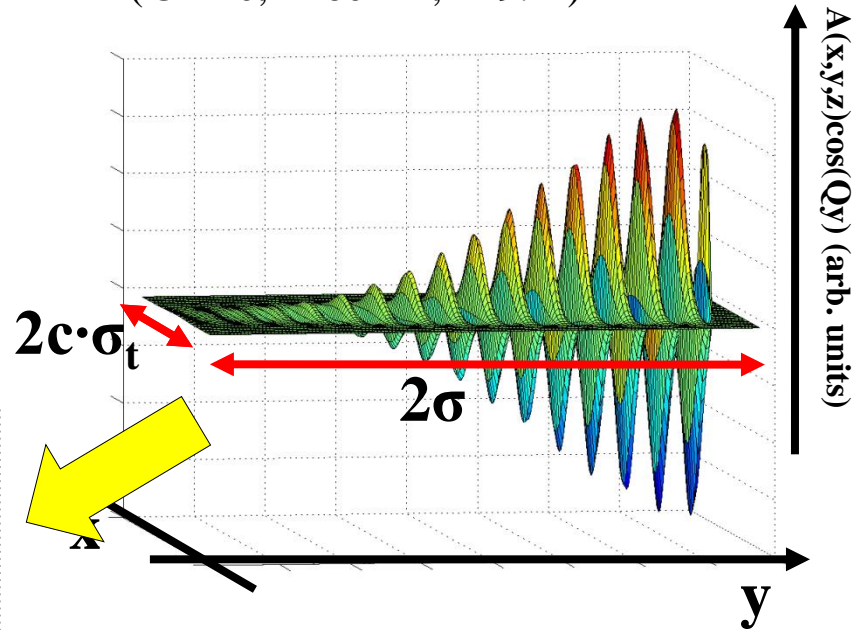
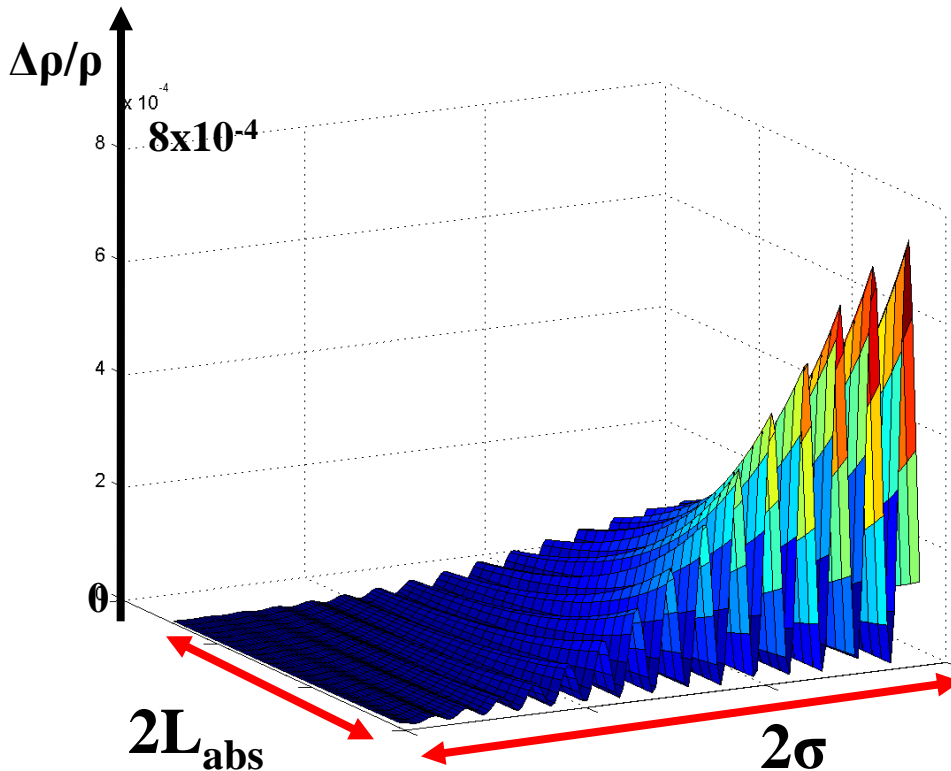


Elettra Sincrotrone Trieste

SiO₂ sample

Relative density variation (@ z=0, considering only the optical absorption of pump radiation)

Interference @ sample position
(@ z=0, λ=60 nm, θ=9.2°)

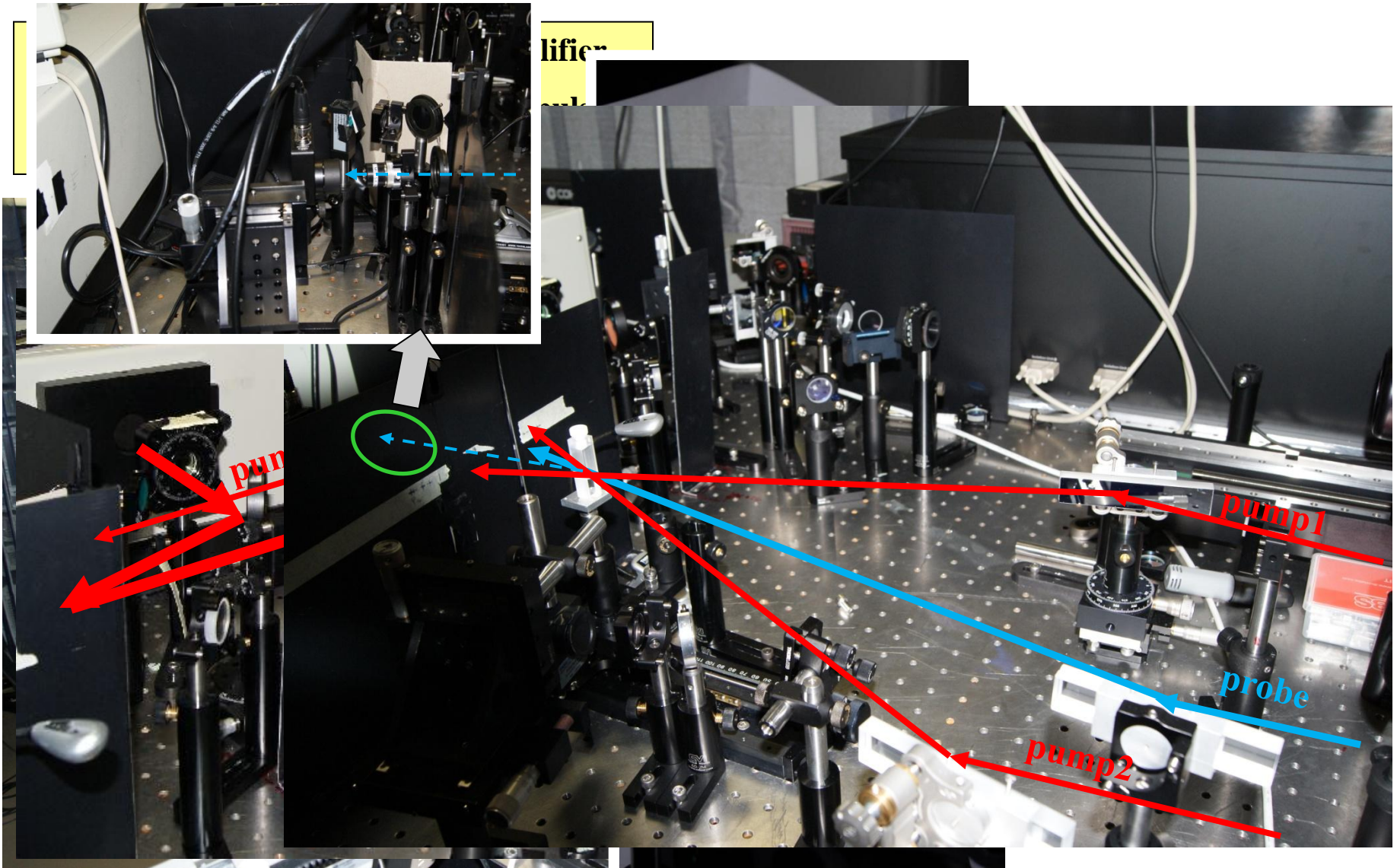


$$\Delta\rho/\rho(x,y,z) \sim \alpha \Delta E(x,y,x) / (\Delta V c_v \rho)$$

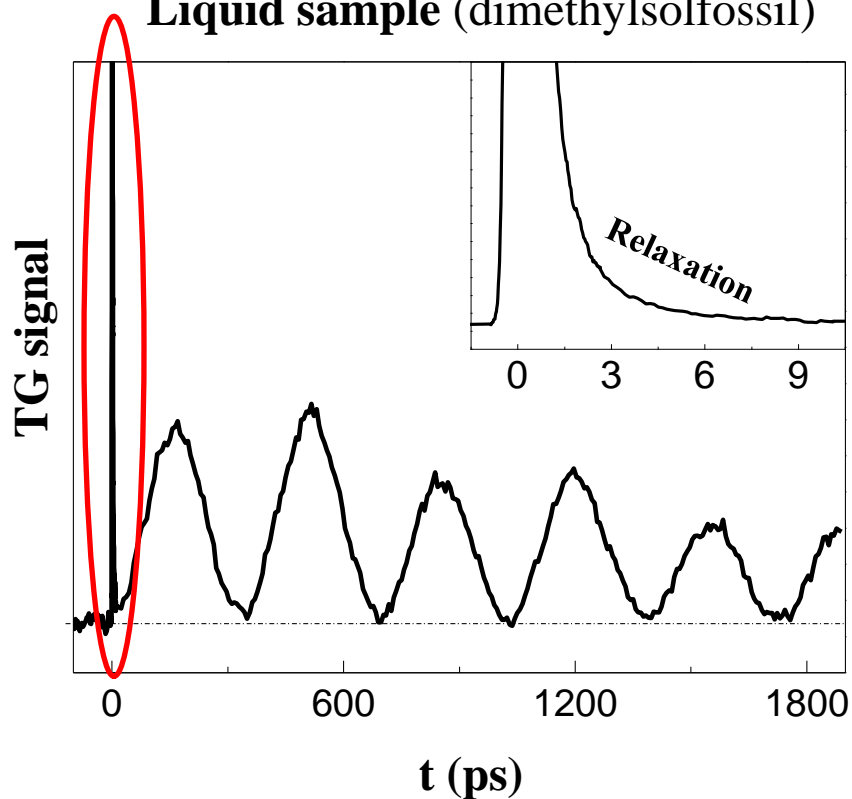
\downarrow $25.5 \cdot 10^{-6} \text{ K}^{-1}$ \uparrow $840 \text{ J kg}^{-1} \text{ K}^{-1}$
 \downarrow 2200 kg m^{-3}

Adiabatic heating of the sample in the illuminated region < 3 °C

Expected **count rate**: 1 – 10⁴ counts per pulse



Liquid sample (dimethylsolfossil)



Sound velocity = **1486 +/- 2 m/s**

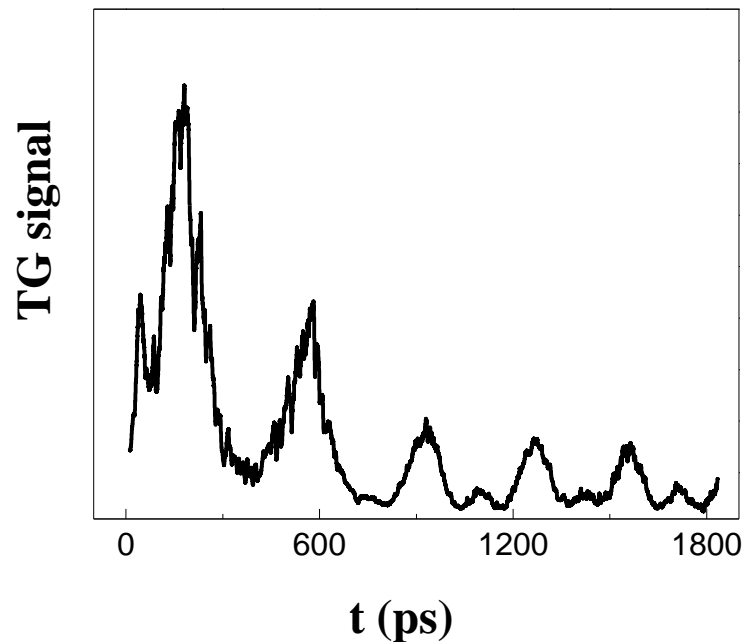
Pump energy ~ 25 $\mu\text{J}/\text{pulse}$

Probe energy ~ 5 $\mu\text{J}/\text{pulse}$

Beam dimensions ~ 50÷200 μm

$\theta = 26^\circ$, $\Delta t = 150 \text{ fs}$, $\lambda = 800 \text{ nm}$

Surface (200 nm Au on Si)

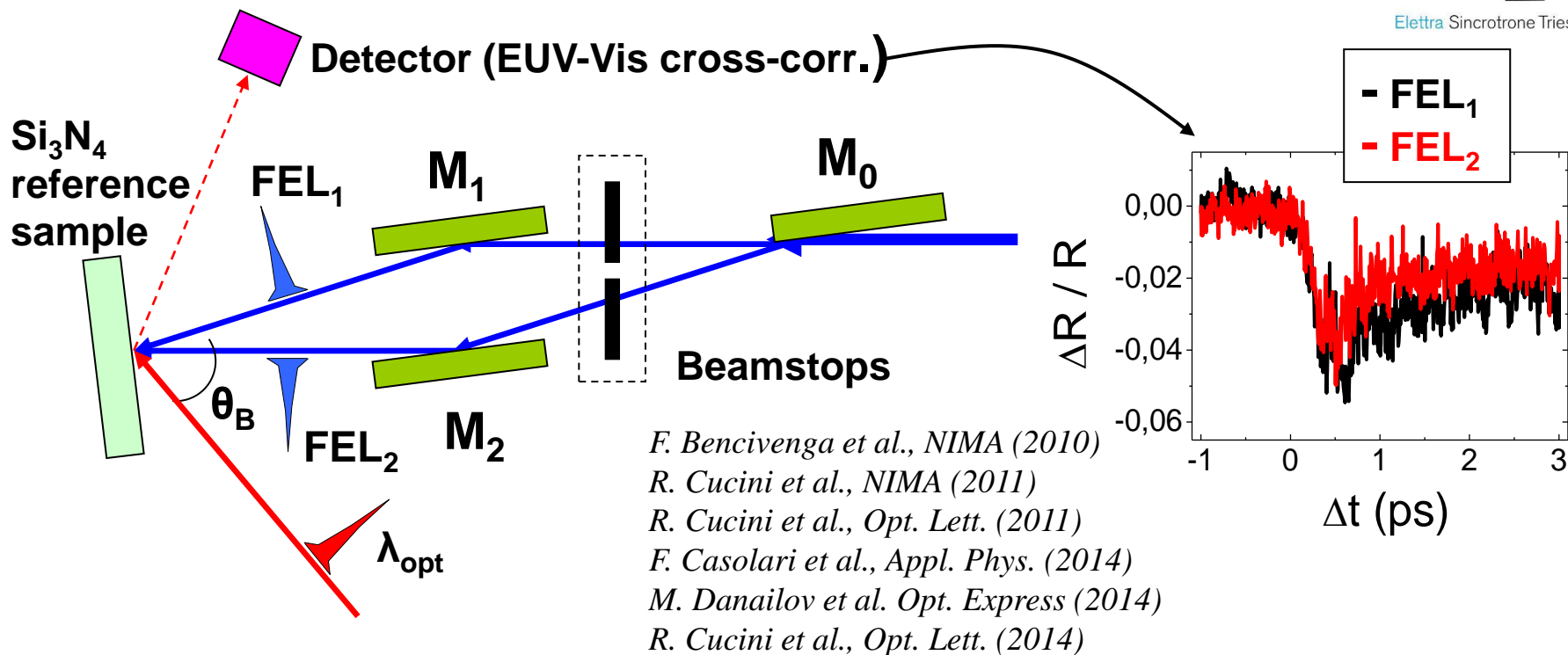


R. Cucini et al et al., Opt. Lett (2011)

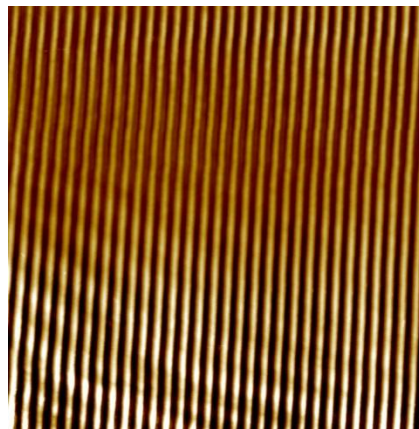
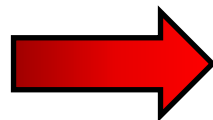
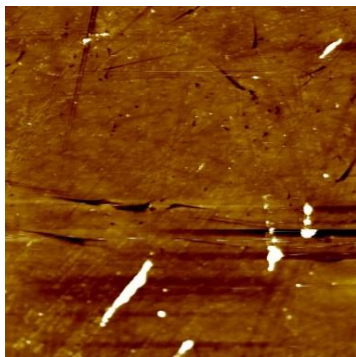
Transient Grating Experiments on V-SiO₂



Elettra Sincrotrone Trieste



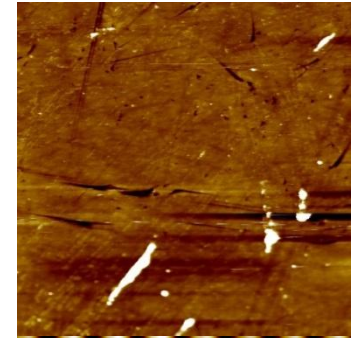
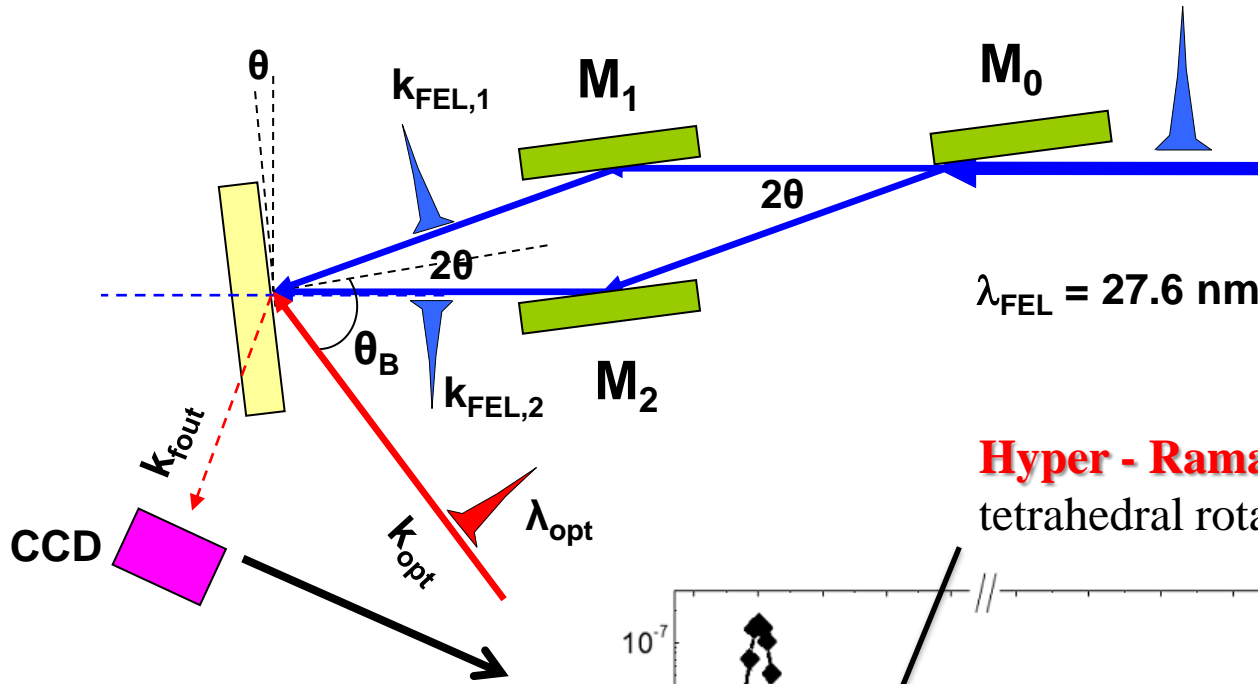
V-SiO₂ sample



Permanent gratings on SiO₂ (after 1000's shots @ FEL flux > 50 mJ/cm²)

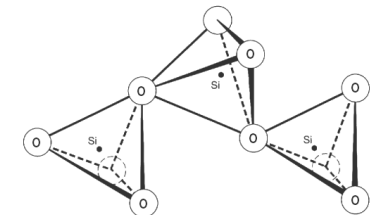
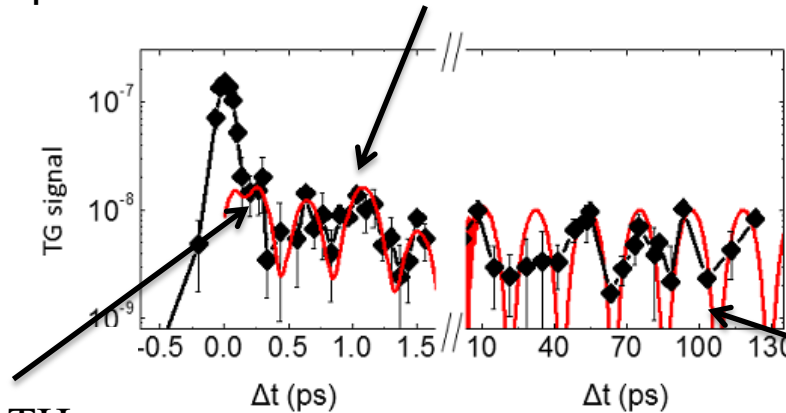
Four-wave mixing experiments with extreme ultraviolet transient gratings

F. Bencivenga et al., Nature 2015



Hyper-Raman modes \rightarrow coupled tetrahedral rotations $\nu_2 \approx 4.1$ THz

Raman modes \rightarrow tetrahedral bending $\nu_1 \approx 1.2$ THz

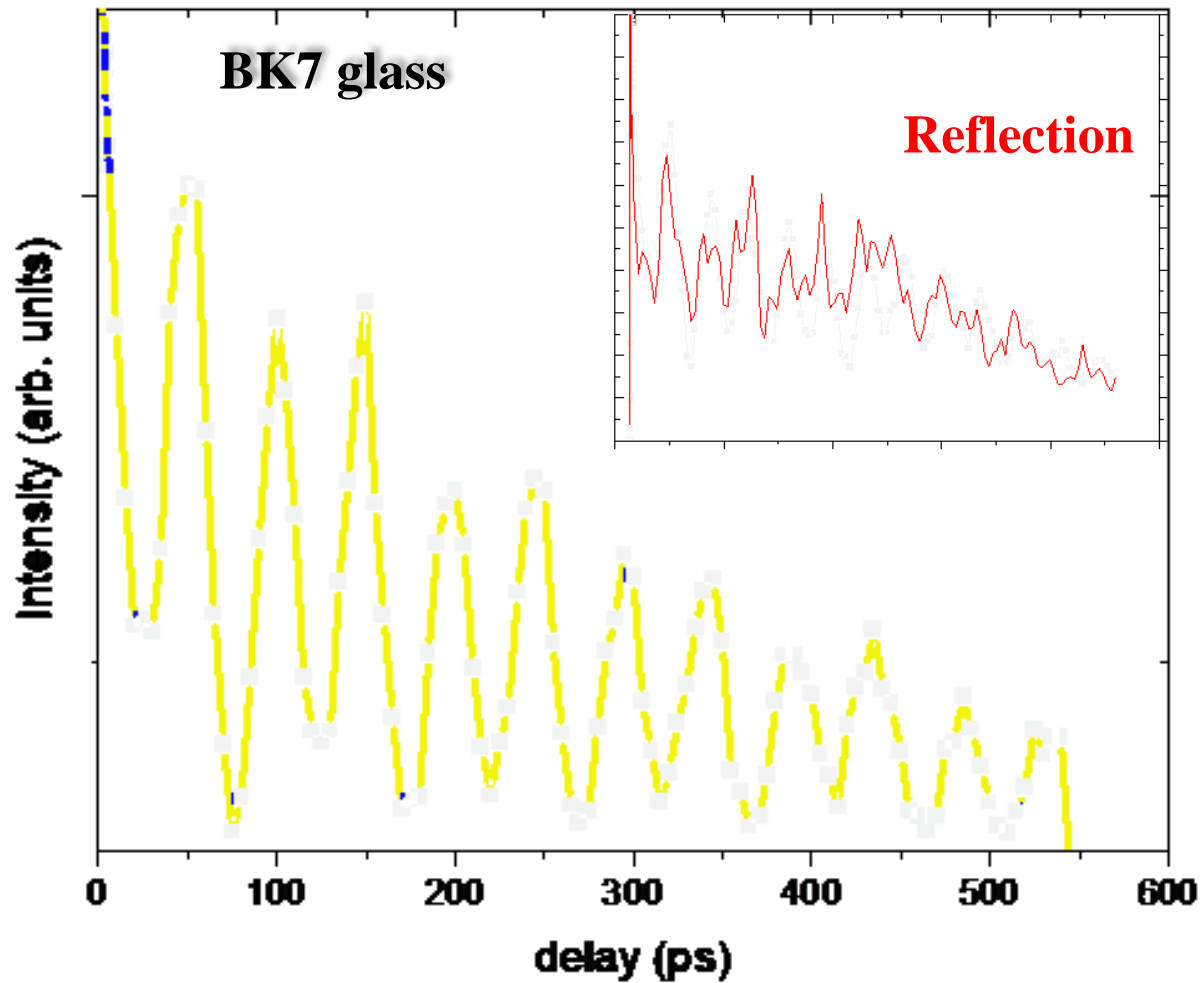


Acoustic-like excitations

After 12 months



Elettra Sincrotrone Trieste



Massachusetts
Institute of
Technology

K. Nelson



PAUL SCHERRER INSTITUT

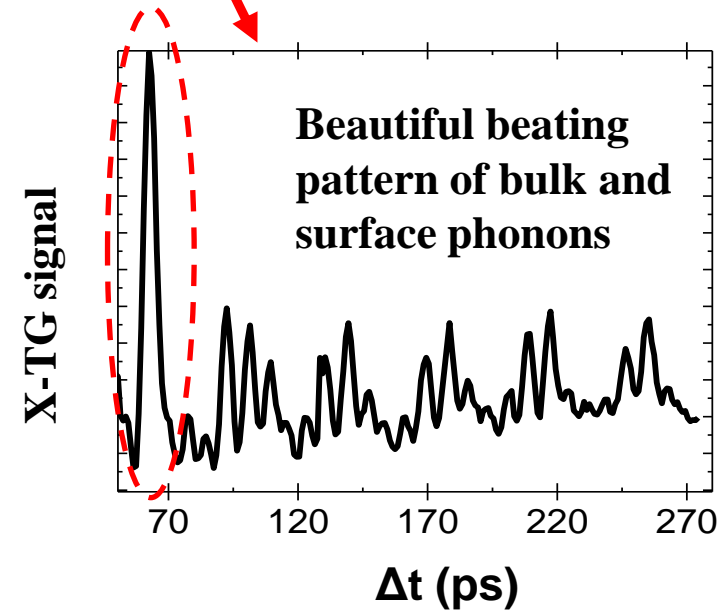
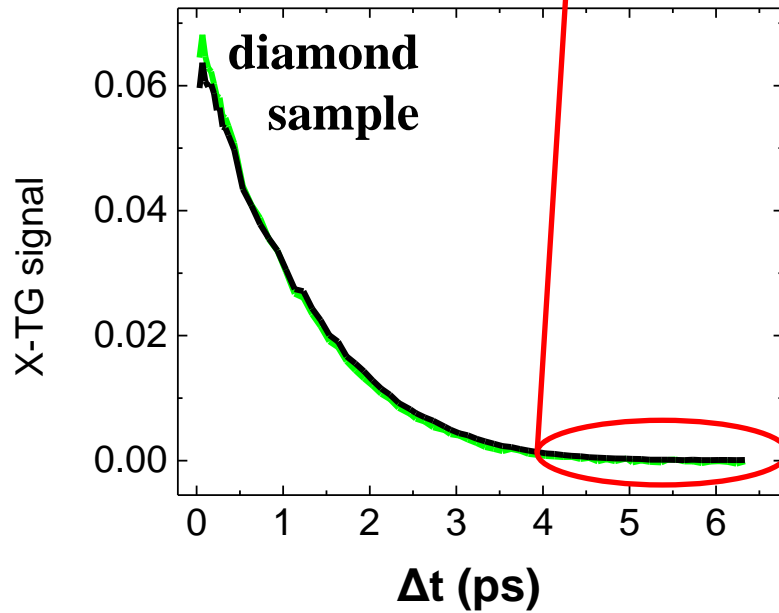
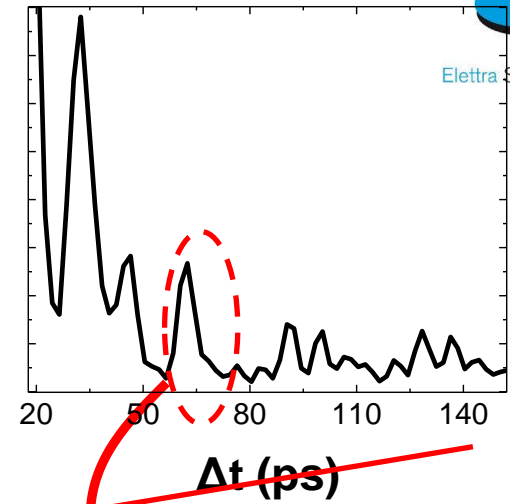
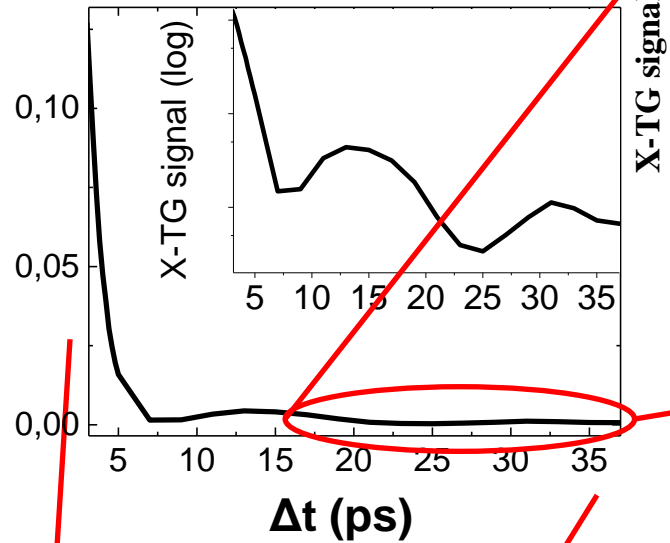


G. Knopp



G. Monaco

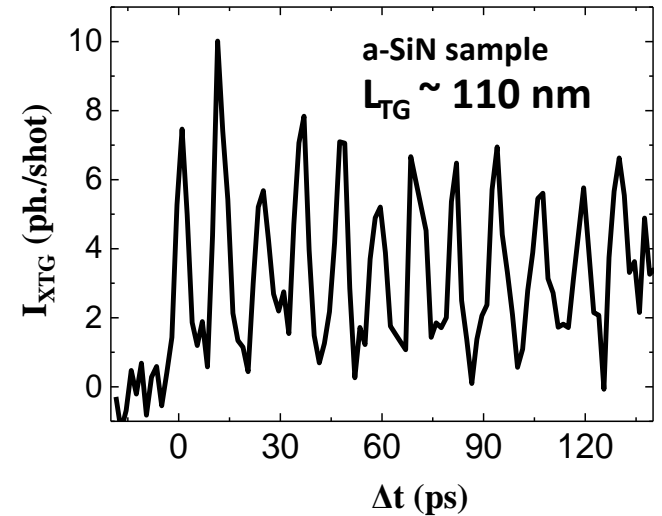
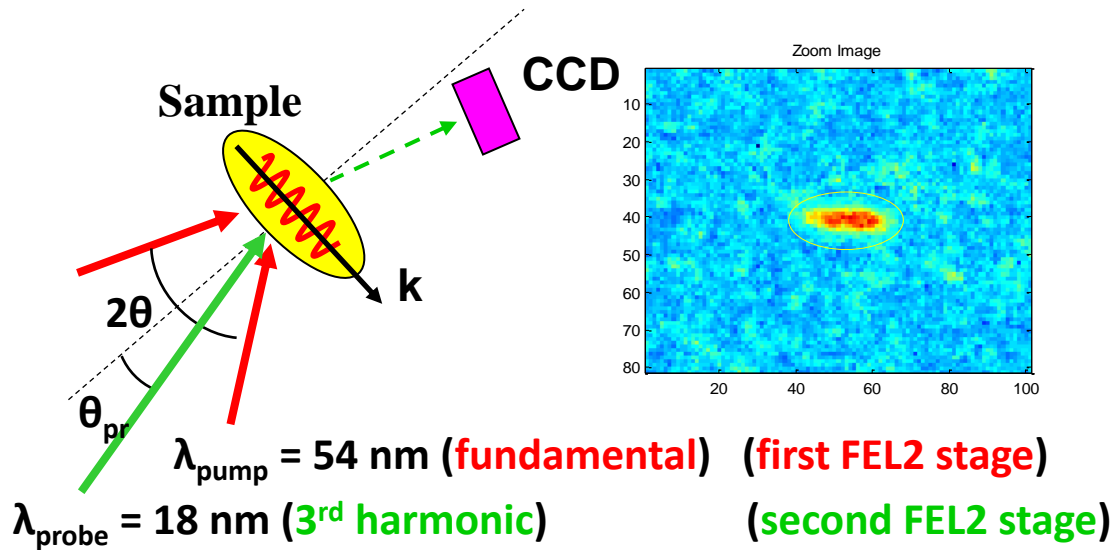
The Contrast



TIMER - All EUV pulses

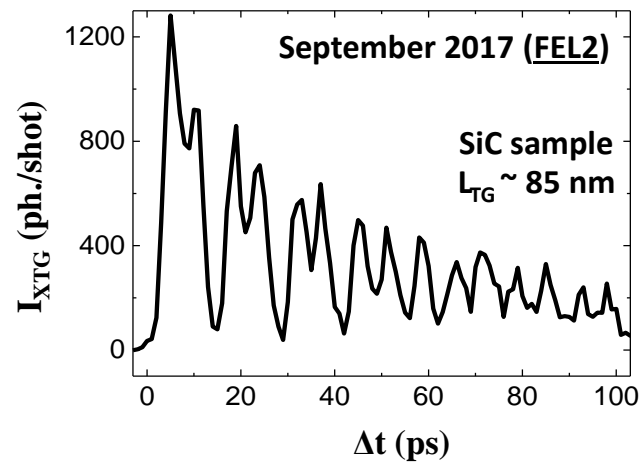
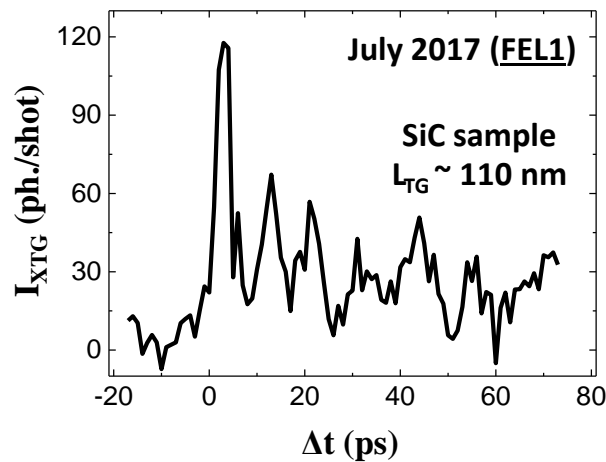


Elettra Sincrotrone Trieste



FEL1 (fundamental + 3rd harmonic)

FEL2 (fundamental of 1st and 2nd stage)

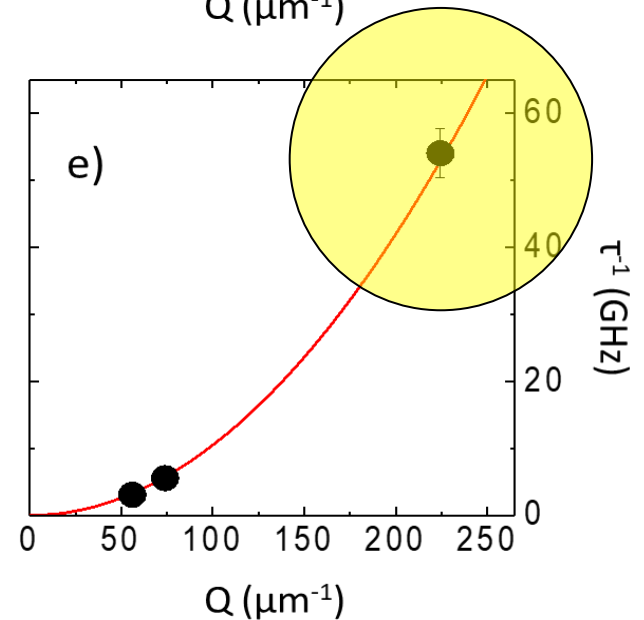
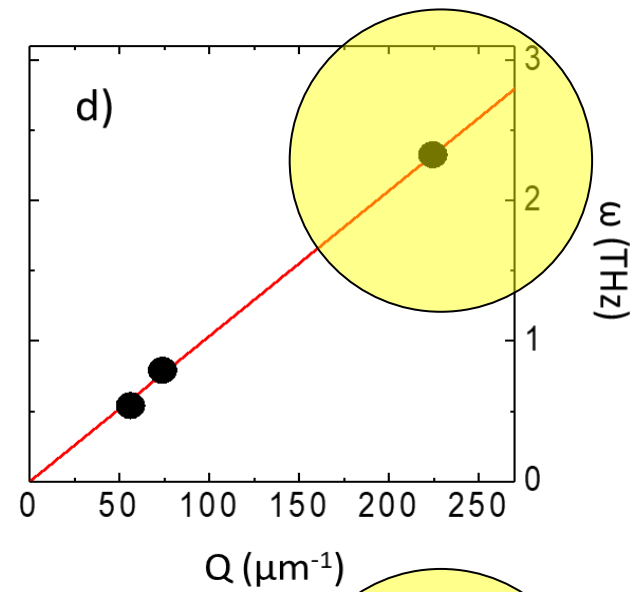
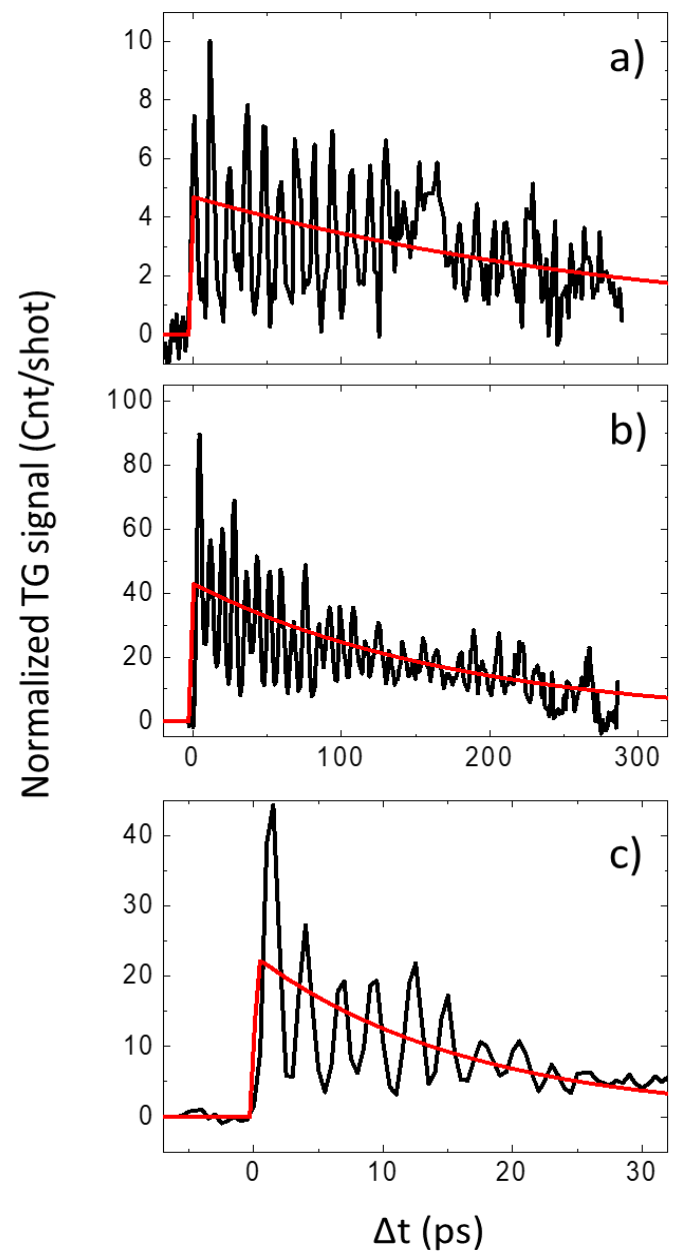


Acoustic modes in disordered systems at the nanoscale



Elettra Sincrotrone Trieste

a-SiN sample



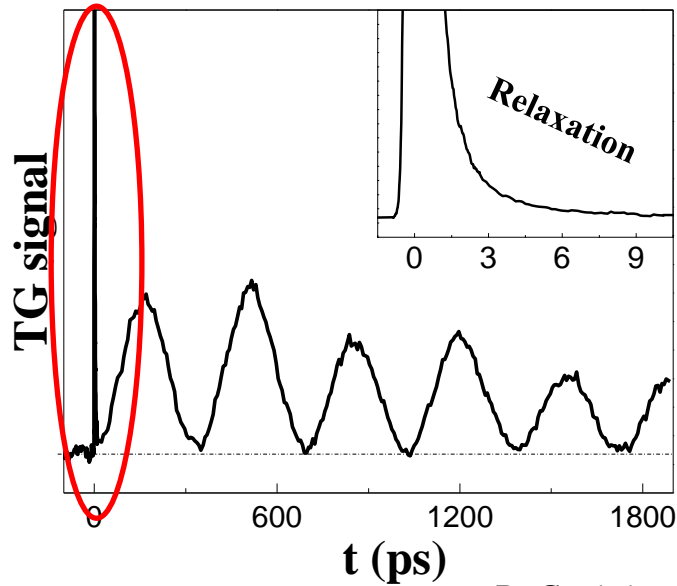
F. Bencivenga et al., in preparation

Diffusion Phenomena with TG



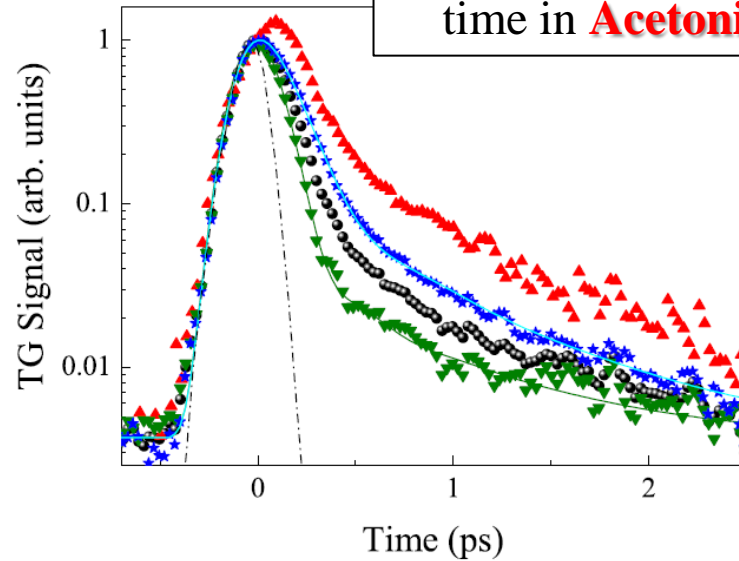
Elettra Sincrotrone Trieste

Liquid sample (**dimethylsolfossil**)

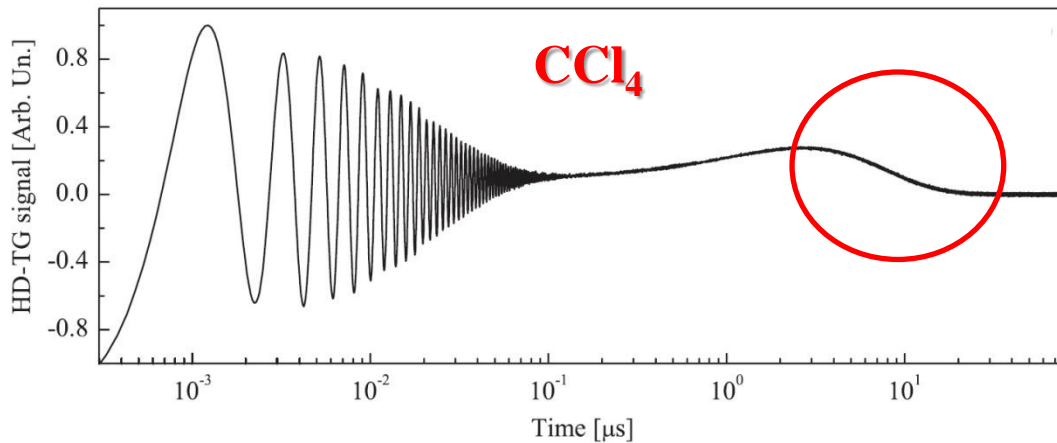


R. Cucini et al., Opt. Lett. 2011

T-dependence relaxation time in **Acetonitrile**



R. Cucini et al., Opt. Lett. 2014

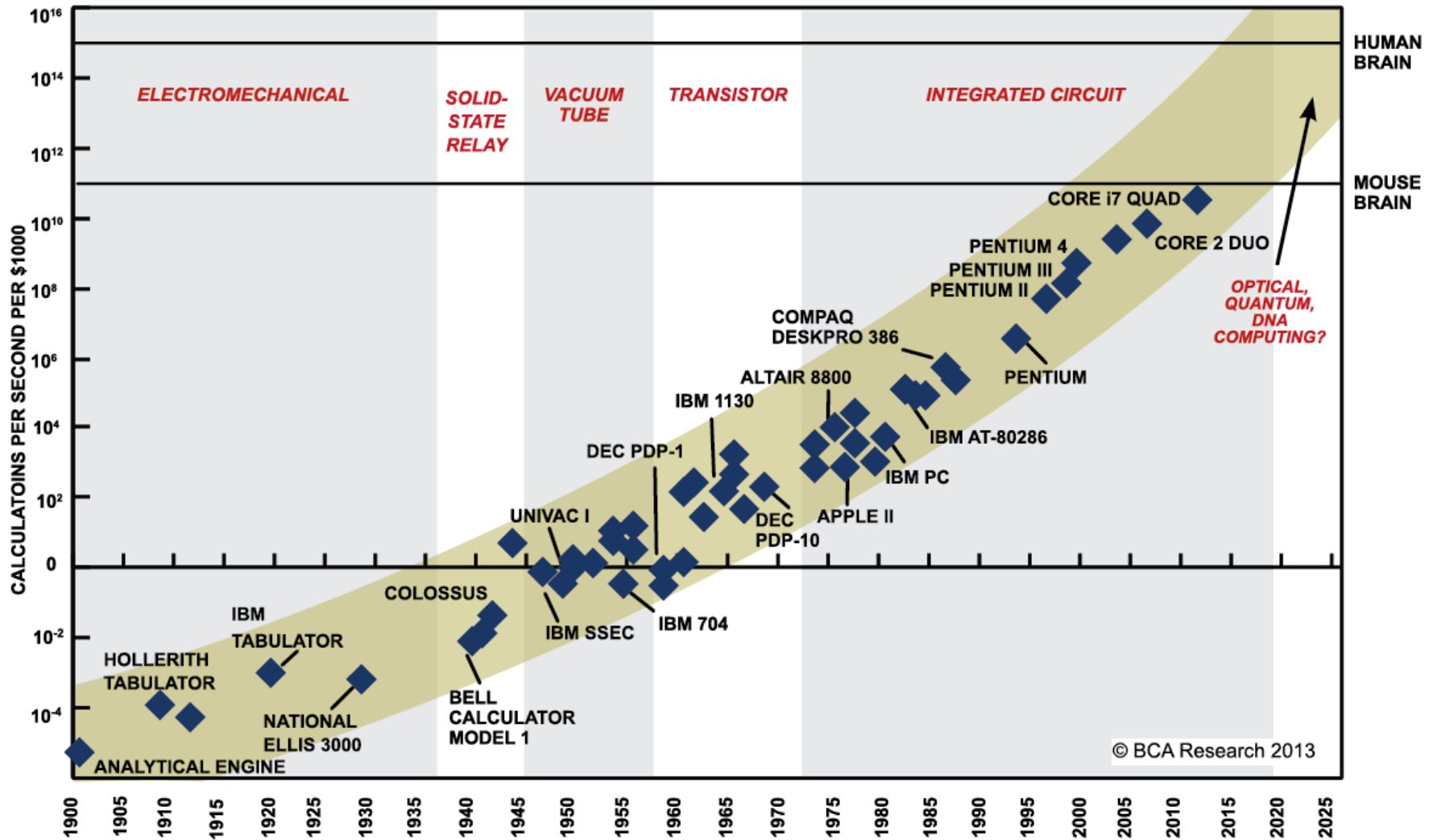


Thermal diffusion \rightarrow
The grating is **washed out**

Smaller and Faster

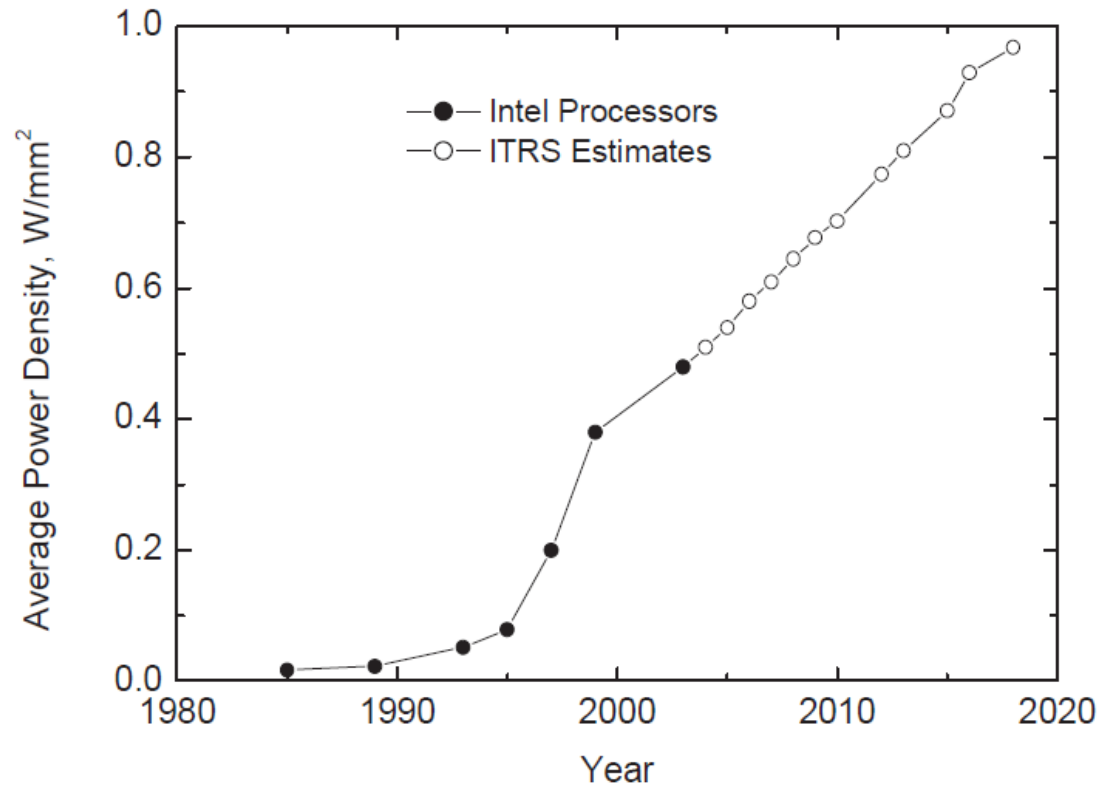


Elettra Sincrotrone Trieste



SOURCE: RAY KURZWEIL, "THE SINGULARITY IS NEAR: WHEN HUMANS TRANSCEND BIOLOGY", P.67, THE VIKING PRESS, 2006. DATAPOINTS BETWEEN 2000 AND 2012 REPRESENT BCA ESTIMATES.

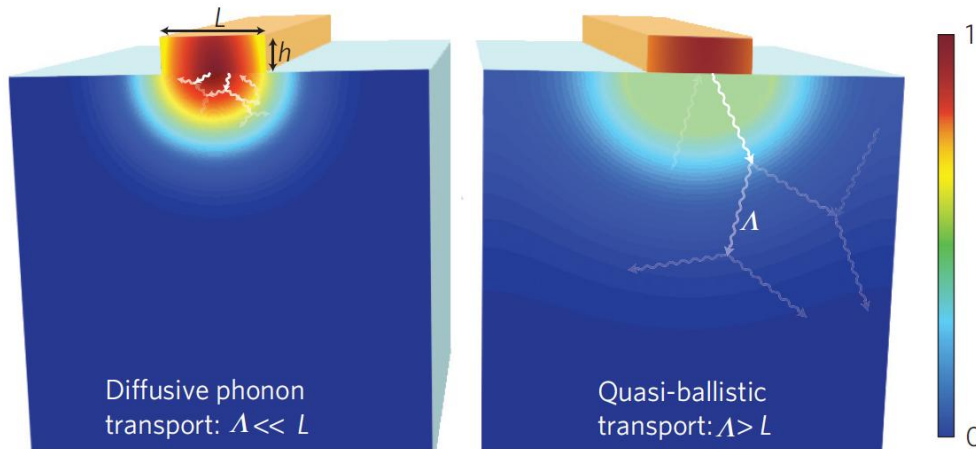
Heat Transport at the Nanoscale



Phonon-mediated **heat transport** at the nanoscale is a hot area of research →
→ thermal management of microelectronic devices and
thermoelectric energy conversion

Heat Transport at the Nanoscale

Phonon **heat transport** in the ballistic regime is unknown

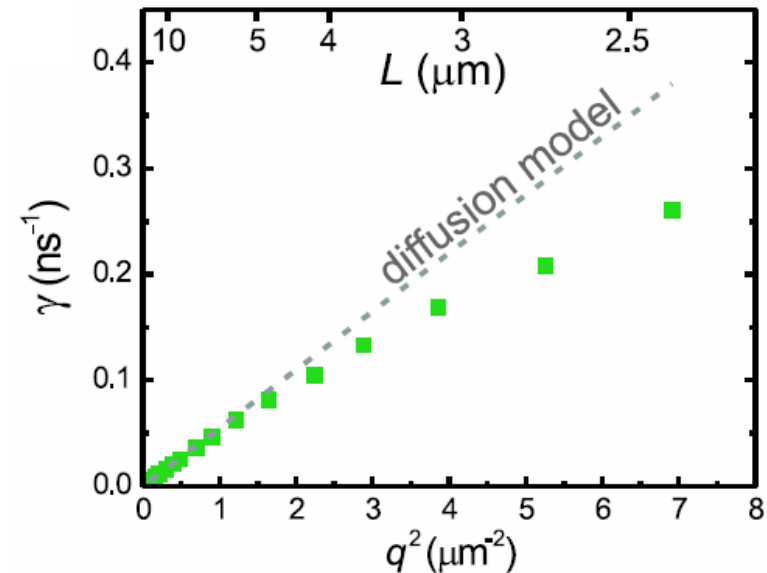


At $\lambda \approx$ to MFP of thermal phonons



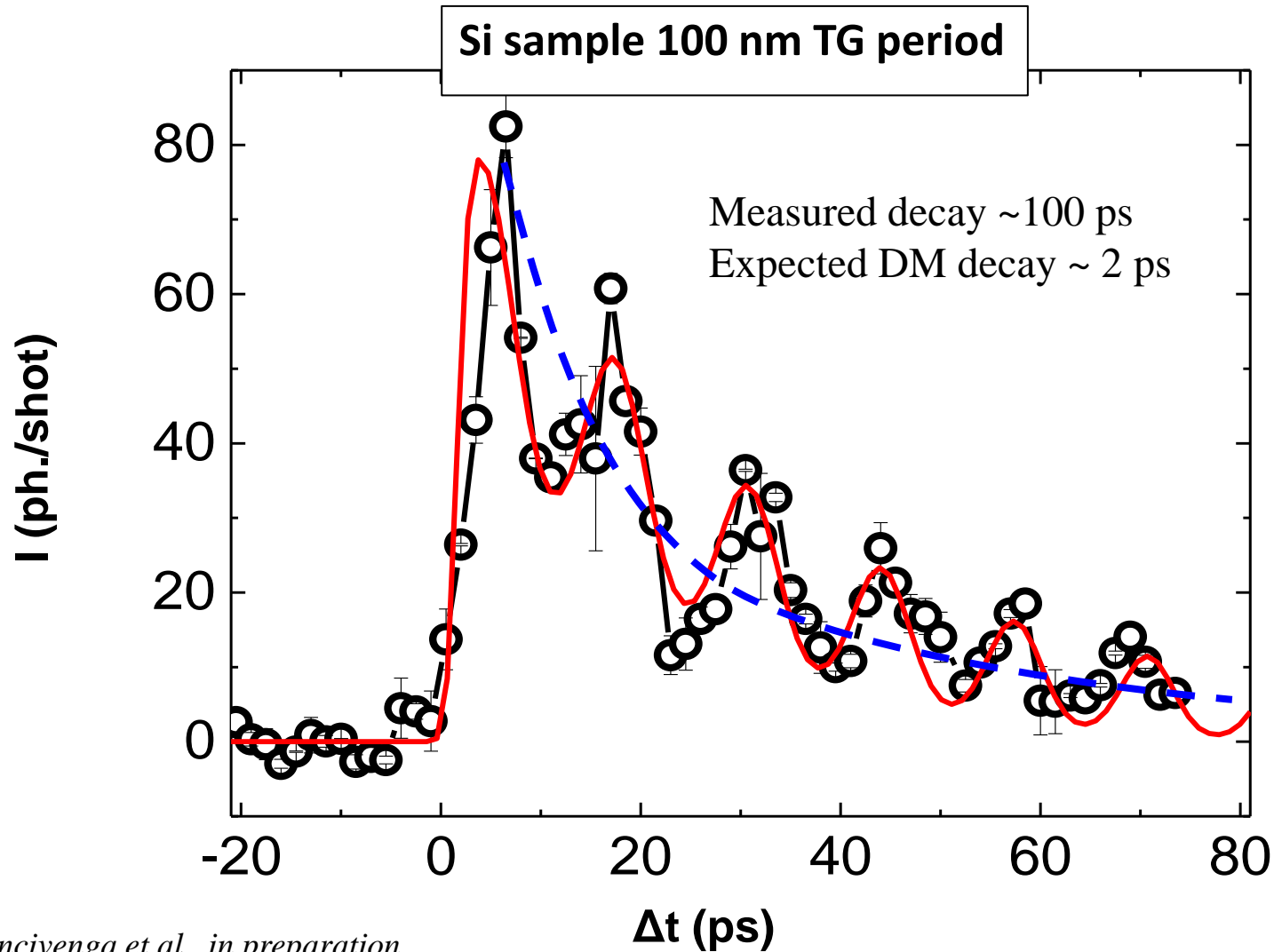
Fourier law breaks down

Deviation from diffusive thermal transport due to **ballistic phonon** in **Si** propagation at distance $\sim \lambda$



J. A. Johnson et al., PRL (2013)

Entering in the Ballistic Regime



F. Bencivenga et al., in preparation

In collaboration with: **K. Nelson, G. Knopp, G. Monaco**

Waterlogged

A midsize data center uses roughly as much water as about 100 acres of almond trees or three average hospitals, and more than two 18-hole golf courses.

Approximate annual water usage, in gallons*



*Use varies depending on climate and other factors

Sources: California Department of Water Resources (orchards); James Hamilton (data centers); U.S. Department of Energy (hospitals); Golf Course Superintendents Association of America (golf courses)

THE WALL STREET JOURNAL.

$$\omega_1 + \omega_2 + \omega_3$$

$$3\omega_j, \omega_j \quad j=1,2,3$$

$$2\omega_i + \omega_j, 2\omega_i - \omega_j, \omega_i - 2\omega_j$$

$$\omega_i + \omega_j - \omega_k, \omega_i - \omega_j - \omega_k$$

PHYSICAL REVIEW

VOLUME 137, NUMBER 3A

1 FEBRUARY 1965

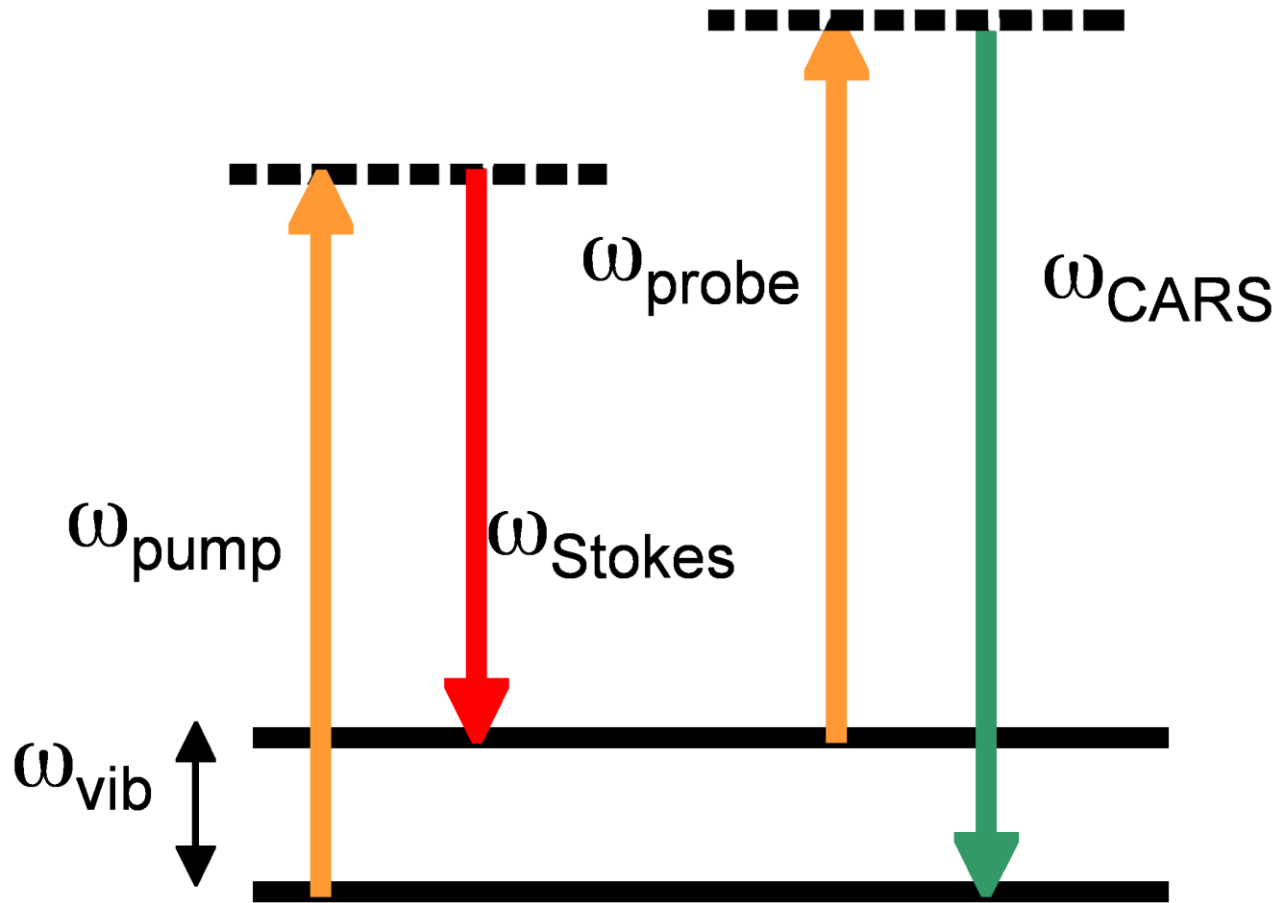
Study of Optical Effects Due to an Induced Polarization Third Order in the Electric Field Strength

P. D. MAKER AND R. W. TERHUNE

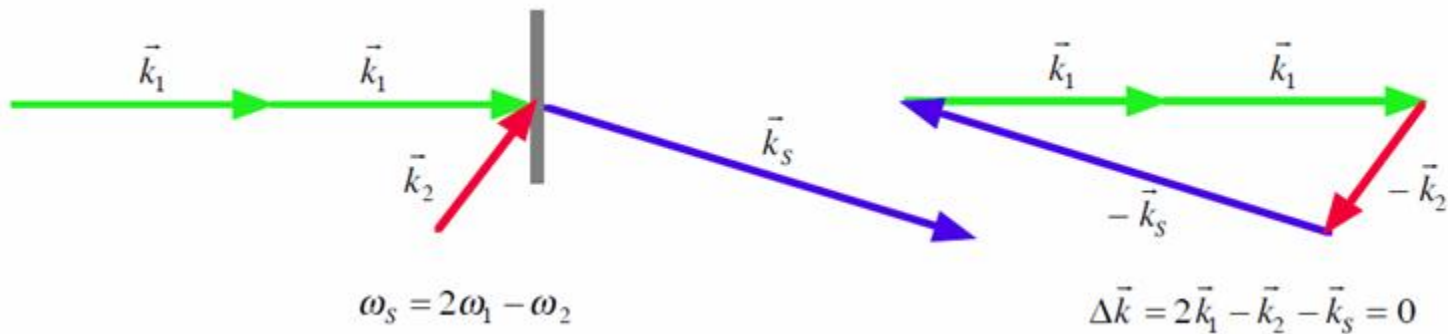
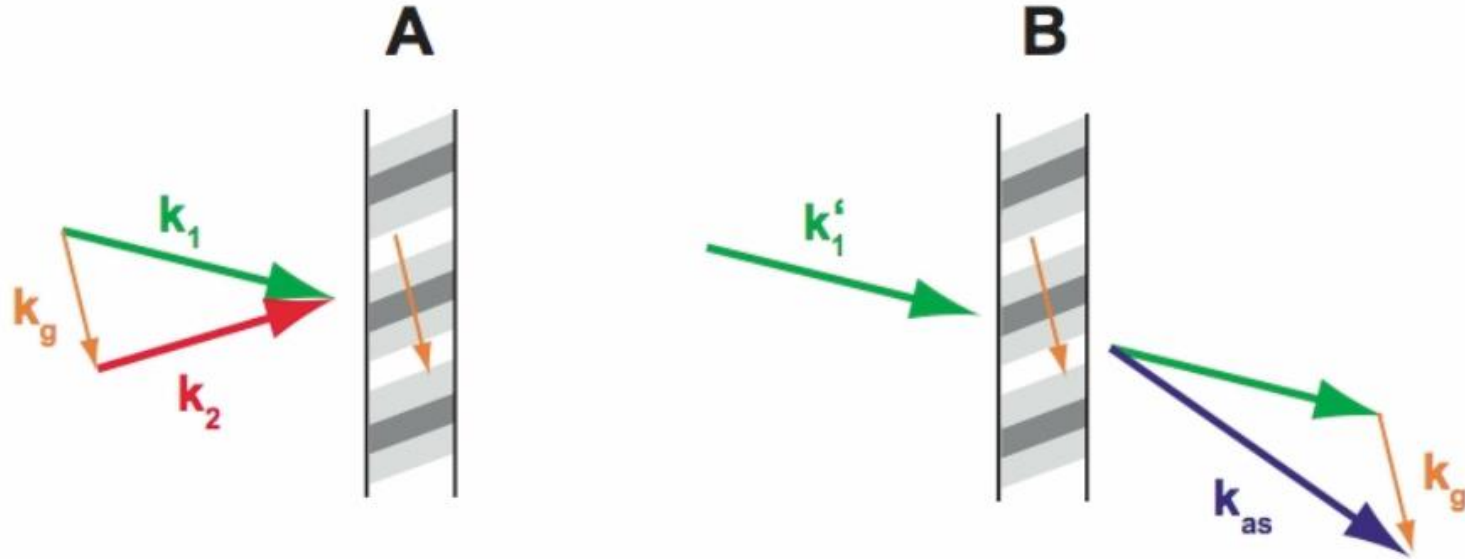
Scientific Laboratory, Ford Motor Company, Dearborn, Michigan

(Received 19 August 1964)

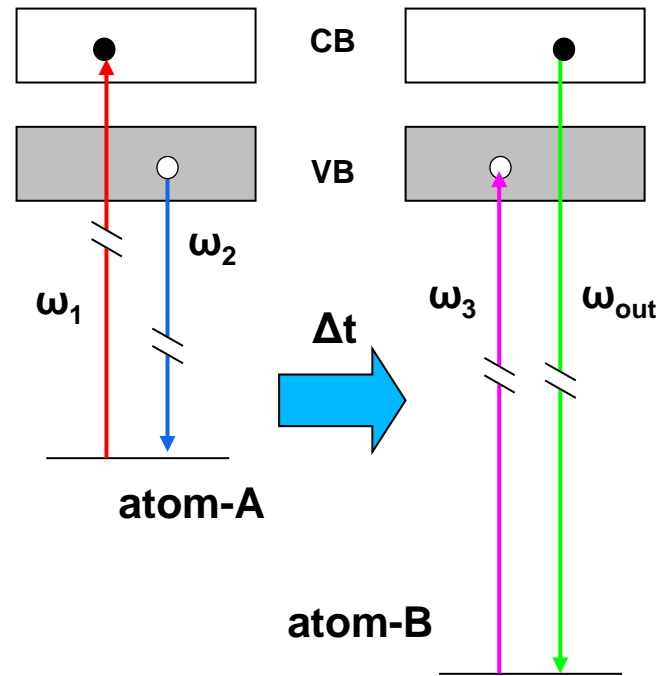
Coherent Antistokes Raman Scattering



Coherent Antistokes Raman Scattering



Resonant CARS



Measure the coherence between the two different sites \rightarrow tuning energies and time delay makes possible to chose where a given excitation is created, as well as where and when it is probed



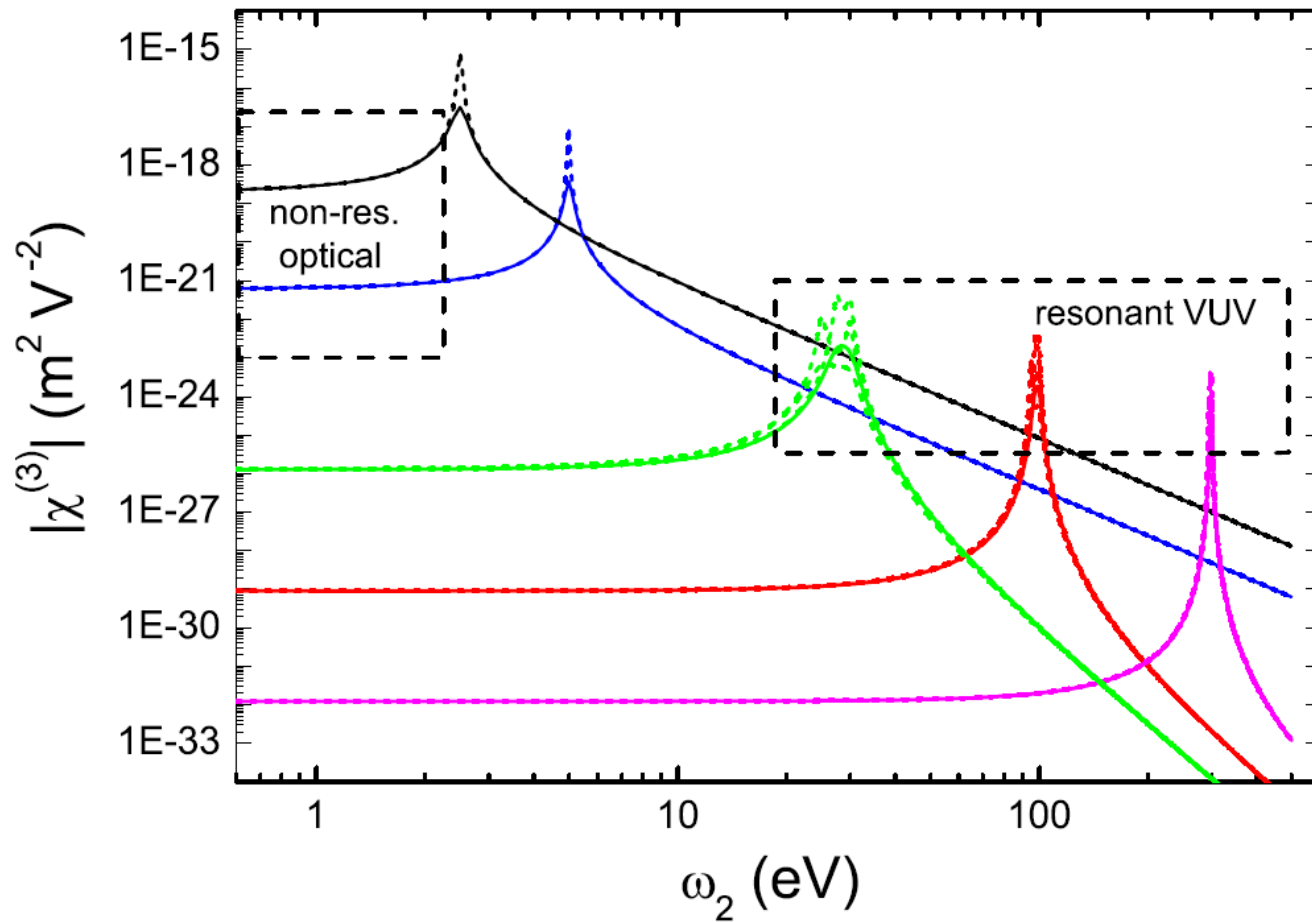
delocalization of electronic states and charge/energy transfer processes.

S. Tanaka and S. Mukamel, PRL (2002)

Exploiting Resonances



Elettra Sincrotrone Trieste



F. Bencivenga et al., New. J. Phys. (2013)

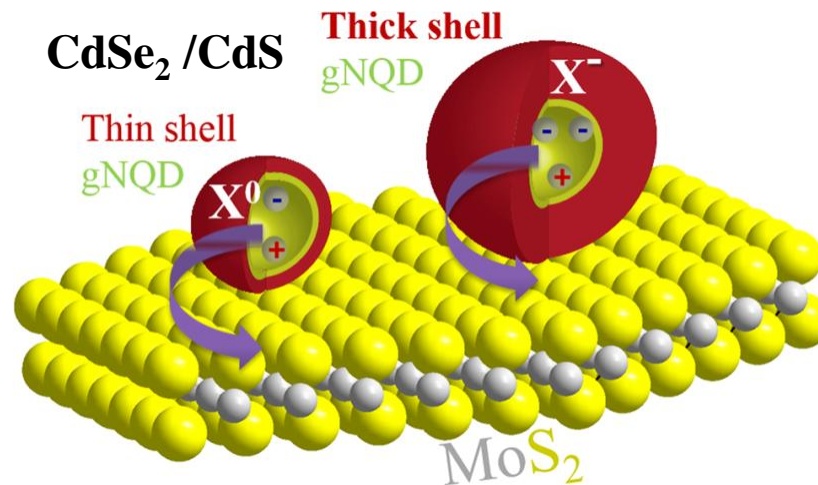
Excitonic Energy Transfer

Energy Transfer from **Giant Semiconductor Nanocrystals** to **MoS₂ Monolayers**

S. Sampat et al., ACS Photonics 2016

2D-transition metal have emerged as a new class of semiconducting materials featuring **high charge carrier mobility** and direct optical band gaps

The strong optical response makes MoS₂ good candidates for: optoelectronic applications (photodetectors), light-emitting diodes, and **solar-harvesting** devices

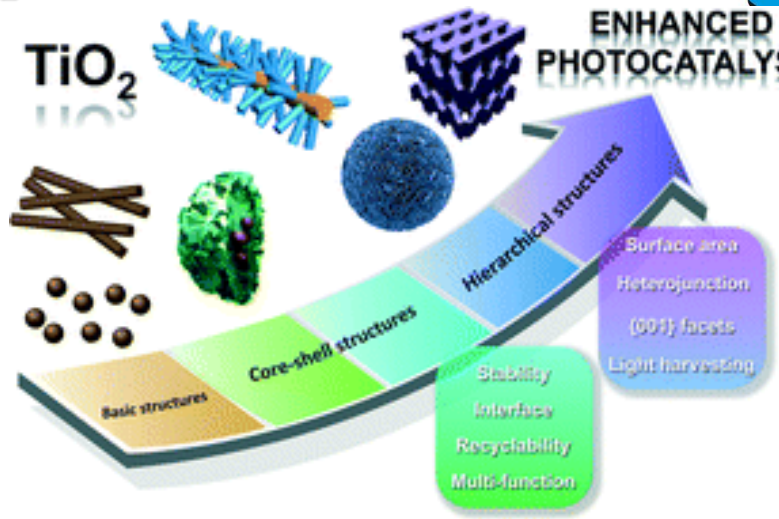


“Slow” ET processes: **1 – 500 ns**

TiO_2

Photocatalysis is a promising ways of exploiting solar radiation for:

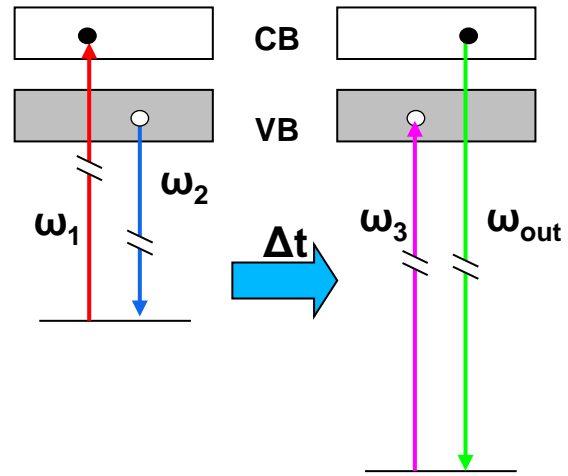
- solar fuels production
- fine chemicals synthesis
- industrial waste removal
- bacterial disinfection
- pollution control



Bandgap engineering of TiO_2 nanostructures \rightarrow to extend light absorption toward the visible region and thus increase the effective catalytic yield

The photocatalytic activity is mostly due to **long lived photo-generated excitons** that act as reductants and oxidants to other species

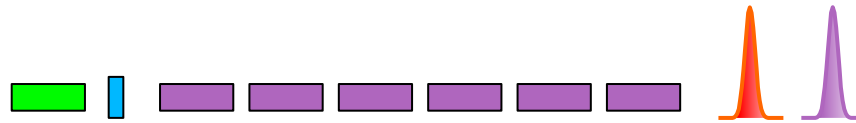
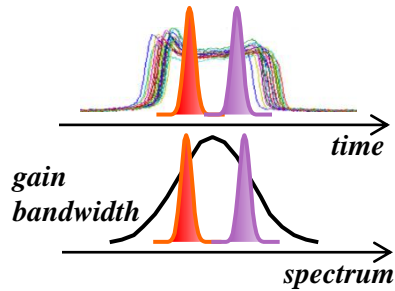
Ti
M edge ~ 34 eV
Lifetime ~ 10 fs



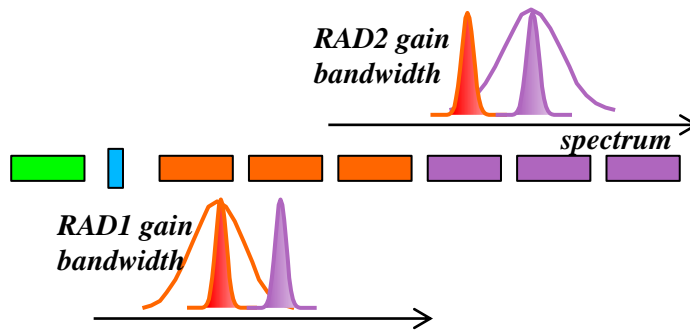
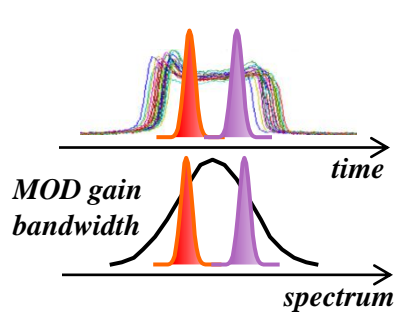
O
K edge ~ 540 eV
Lifetime ~ 8 fs

Multiple Pulse Configurations

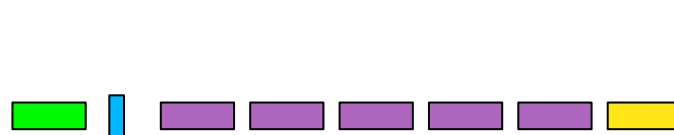
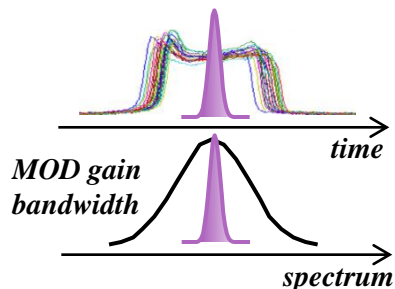
Multiple pulses can be generated by **double pulse seeding**



Spectral separation **0.4-0.7%**
(*E. Allaria et al., Nat. Comm 2013*)

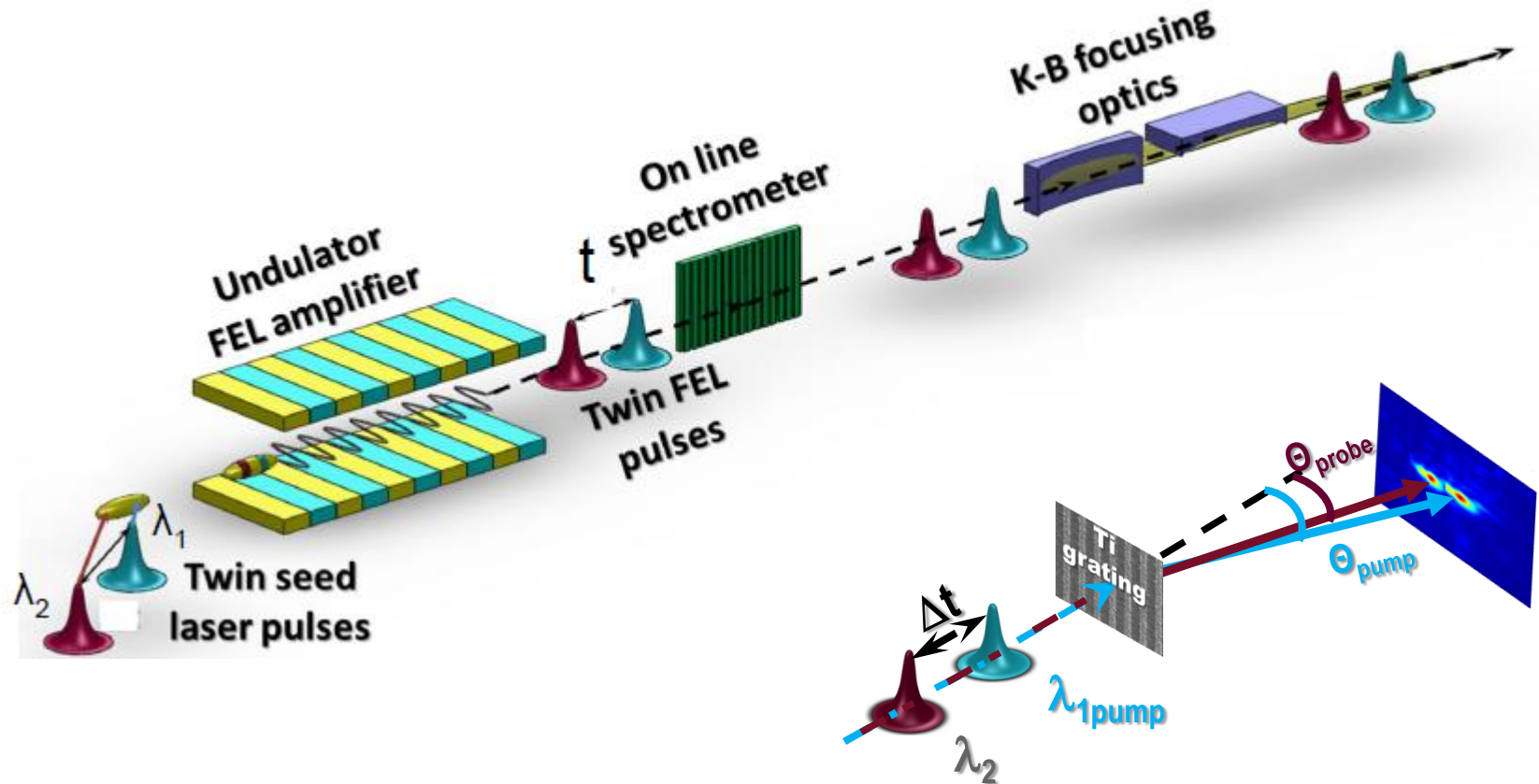


Spectral separation **2-3%**
or much larger if two radiators
are tuned at different harmonics
(*Sacchi et al., Nat. Comm. 2016*)



Two (almost) temporally
superimposed pulses at harmonic
wavelengths of the seed. They are
correlated in phase that can be
controlled with the phase shifter
(*K.C. Prince et al., Nat. Phot.2016*)

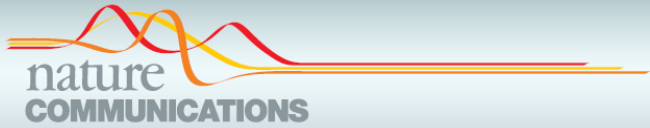
Two-colour pump-probe experiments with a twin-pulse-seed extreme ultraviolet free-electron laser



Element selective magnetization dynamics



Elettra Sincrotrone Trieste



E. Ferrari et al., (2016)

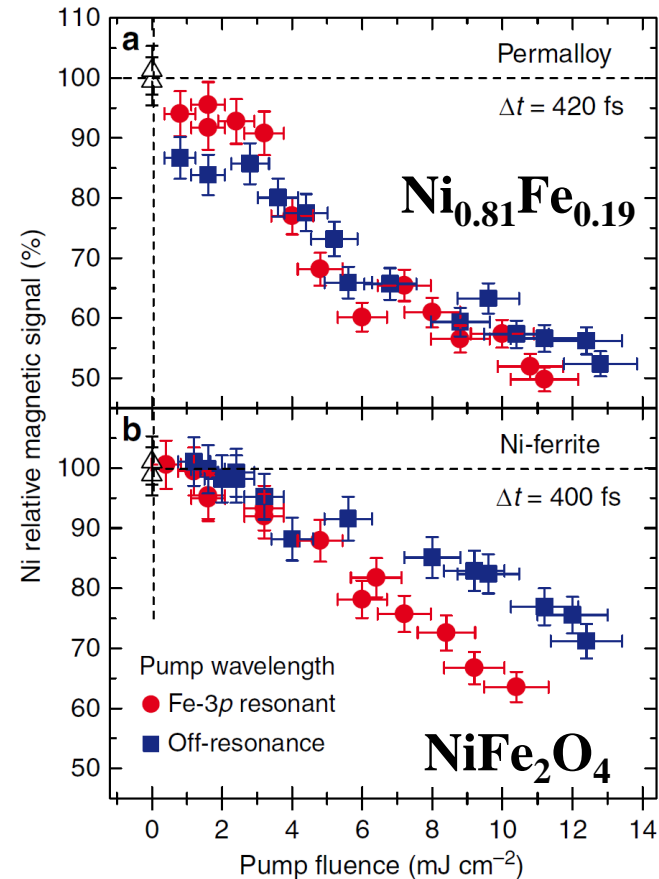
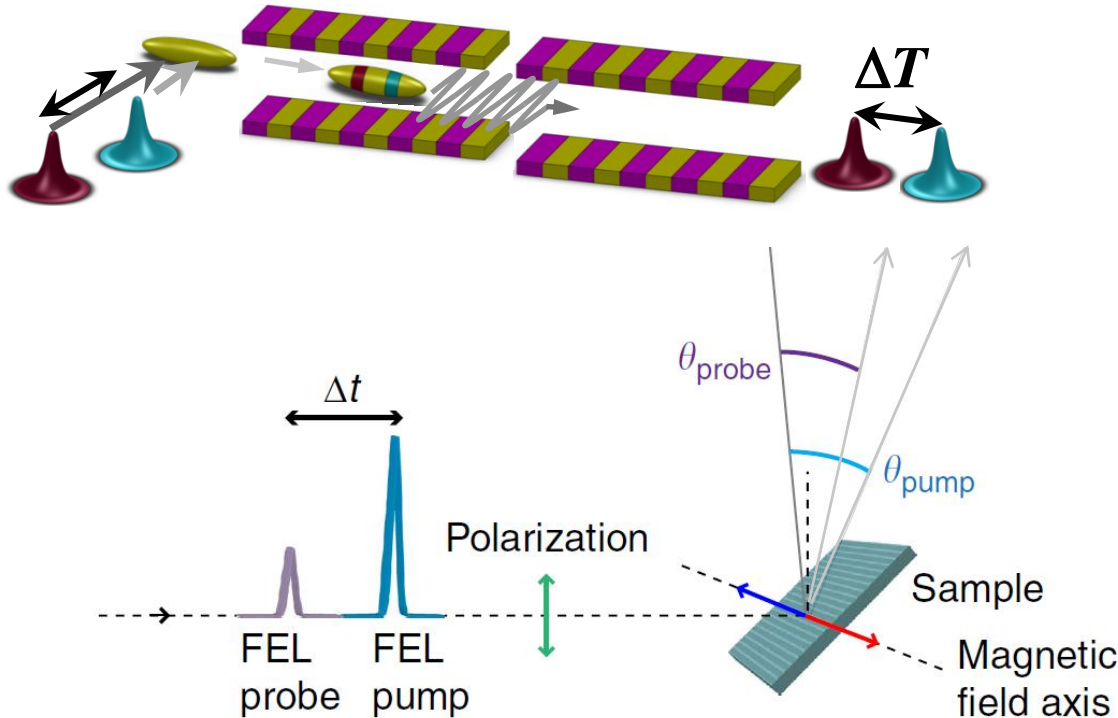
Received 21 Aug 2015 | Accepted 3 Dec 2015 | Published 13 Jan 2016

DOI: 10.1038/ncomms10343

OPEN

Widely tunable two-colour seeded free-electron laser source for resonant-pump resonant-probe magnetic scattering

Radiators at different harmonics



Coherent control with a short-wavelength free-electron laser

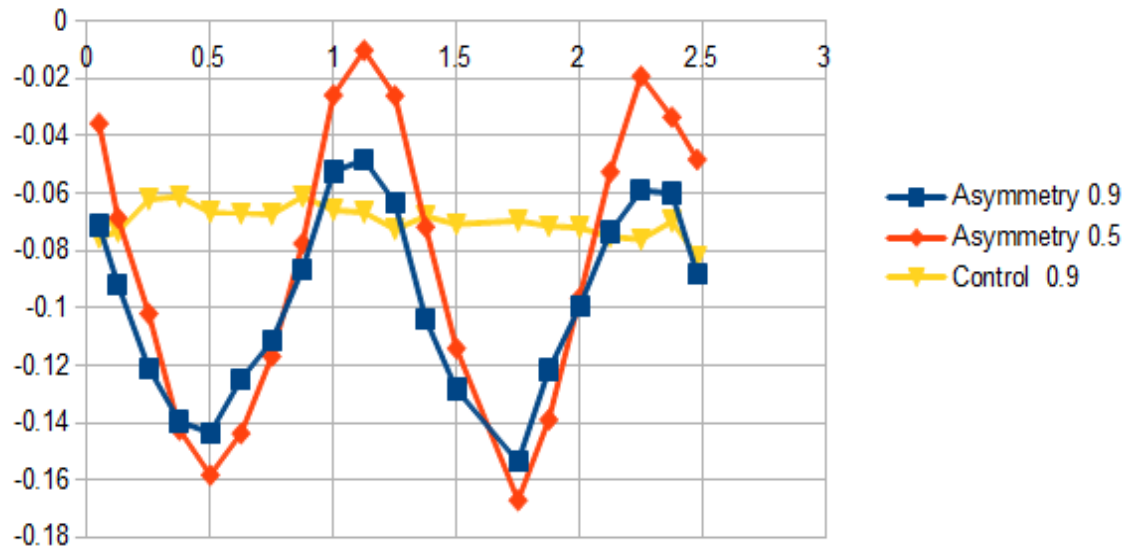
K. Prince et al., (2016)

Interference effect among quantum states using single and multiphoton ionization

C. Chen et al., PRL (1990)

$$\text{Intensity} = |M1 + M2(\phi)|^2 = |M1|^2 + |M2(\phi)|^2 + 2 \text{Re}(M1 M2(\phi))$$

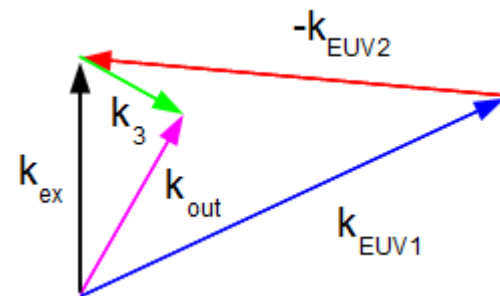
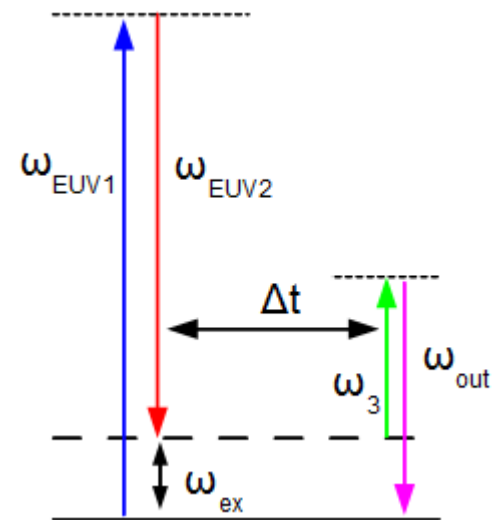
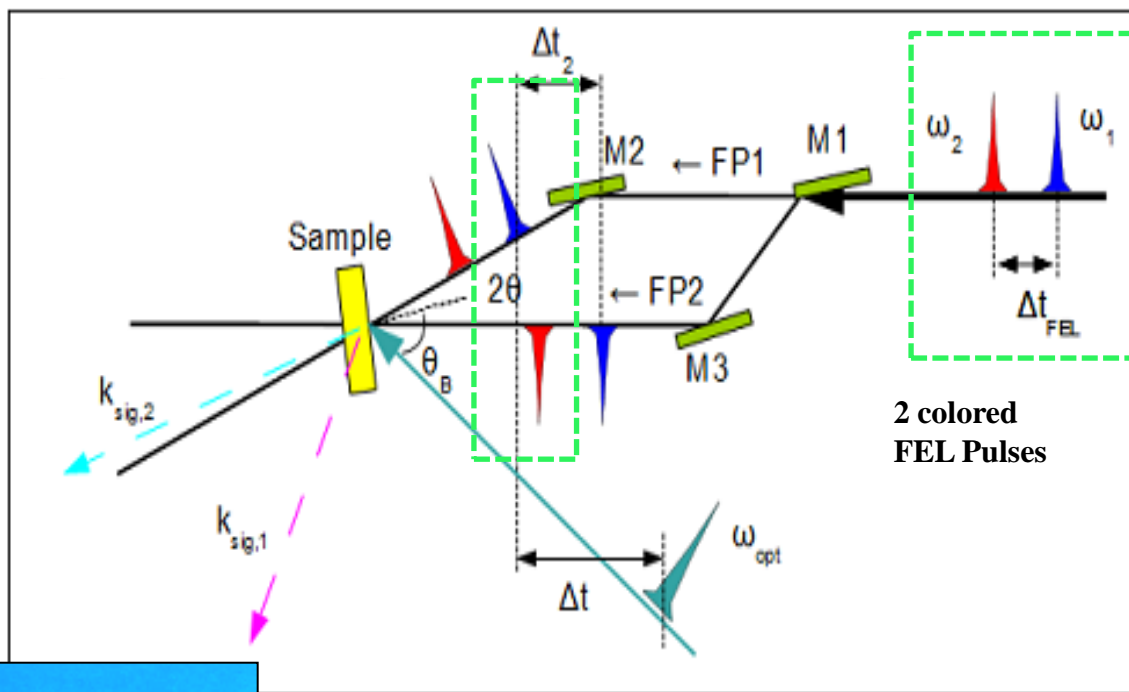
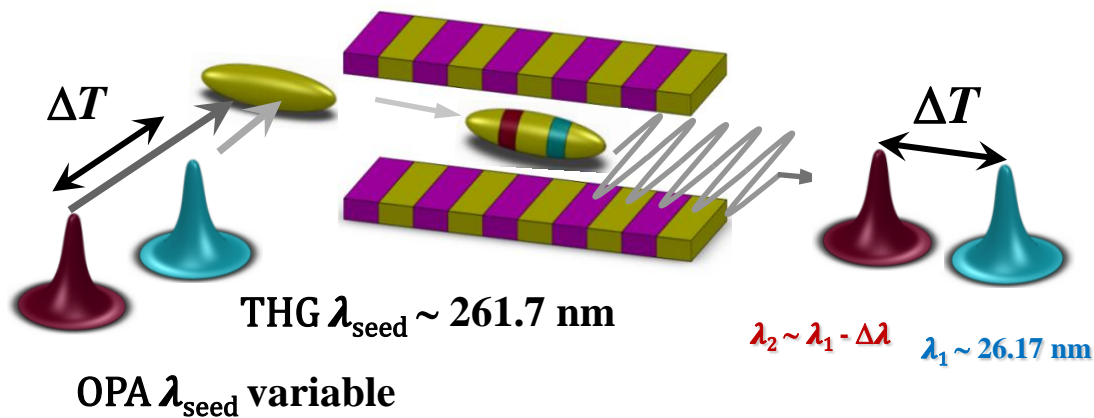
Use of first (62.974 eV) and second harmonic on **2p⁵4s** resonance of Ne



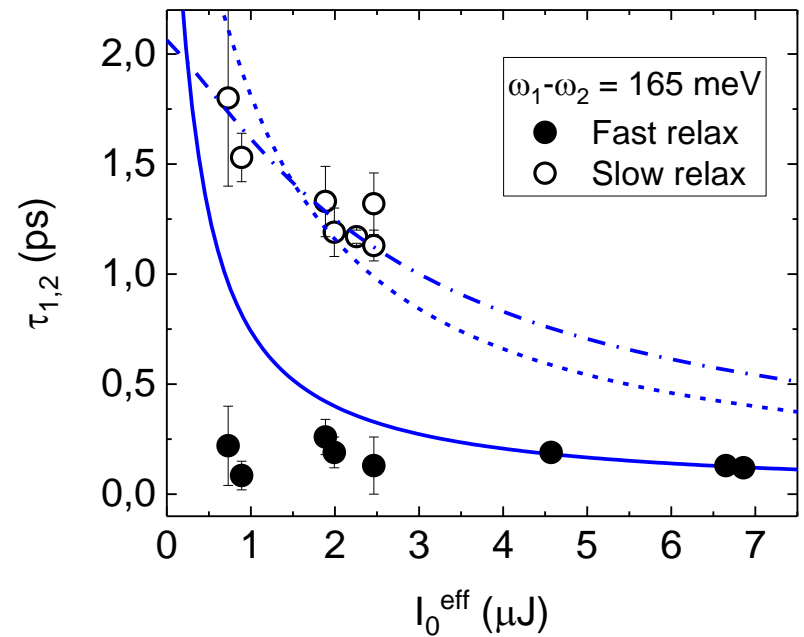
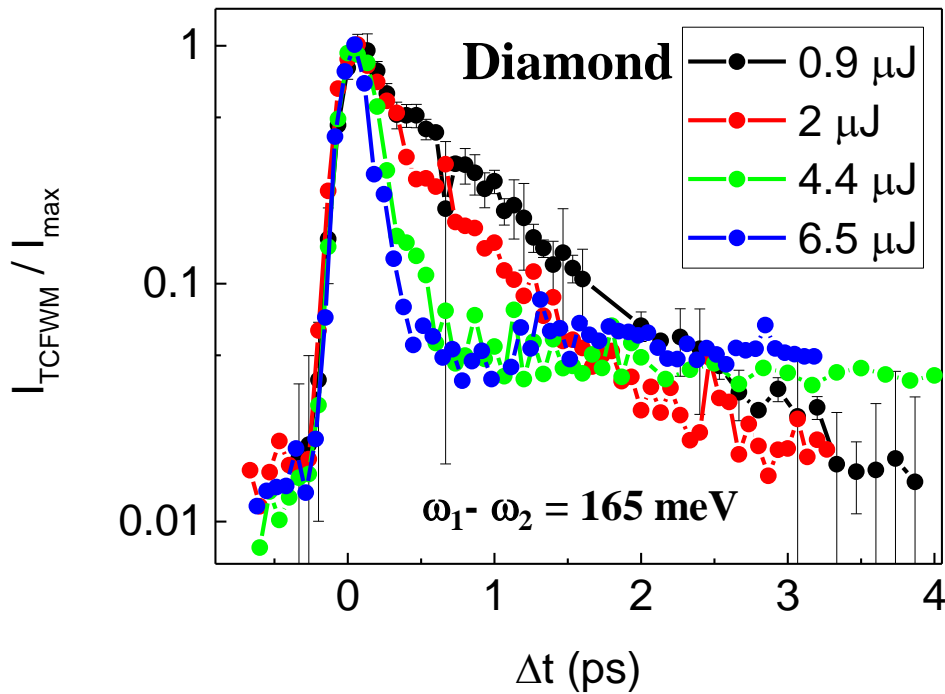
Signal detected as function of phase on the VMI detector

Control of the phase among the two pulses!

FERMI based CARS



F. Bencivenga et al., in preparation



Slow relax \rightarrow expected dephasing time of LO phonons \rightarrow related to the **fraction of non-crystalline** diamond

- transient **amorphization**?
- phonon-plasmon **hybrid modes**?

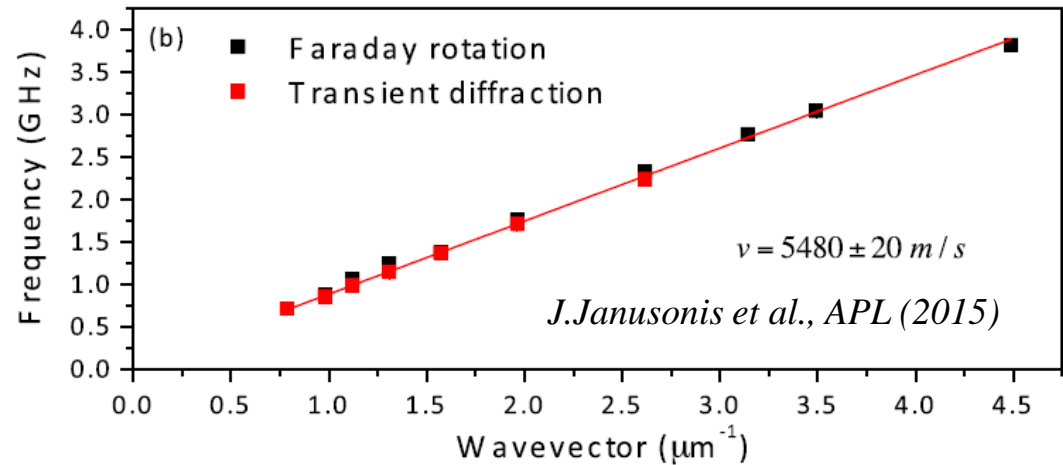
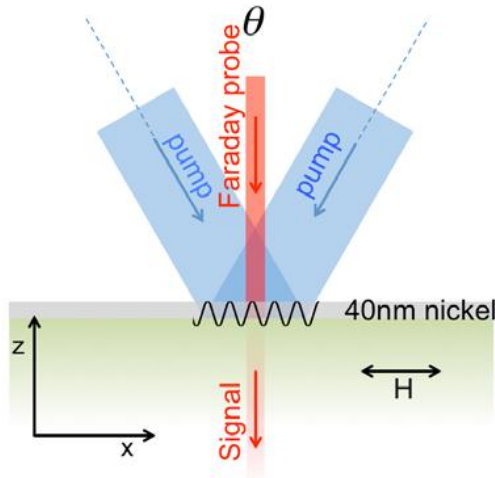
Fast relax \rightarrow **dephasing** of the **electronic excited states** (an hot electron at $\sim 45 \text{ eV}$ plus a valence hole), which is expected to evolve fast ($< 100 \text{ fs}$) through secondary processes (collisions, impact ionization, Auger decay)

Magneto-Elastic Coupling

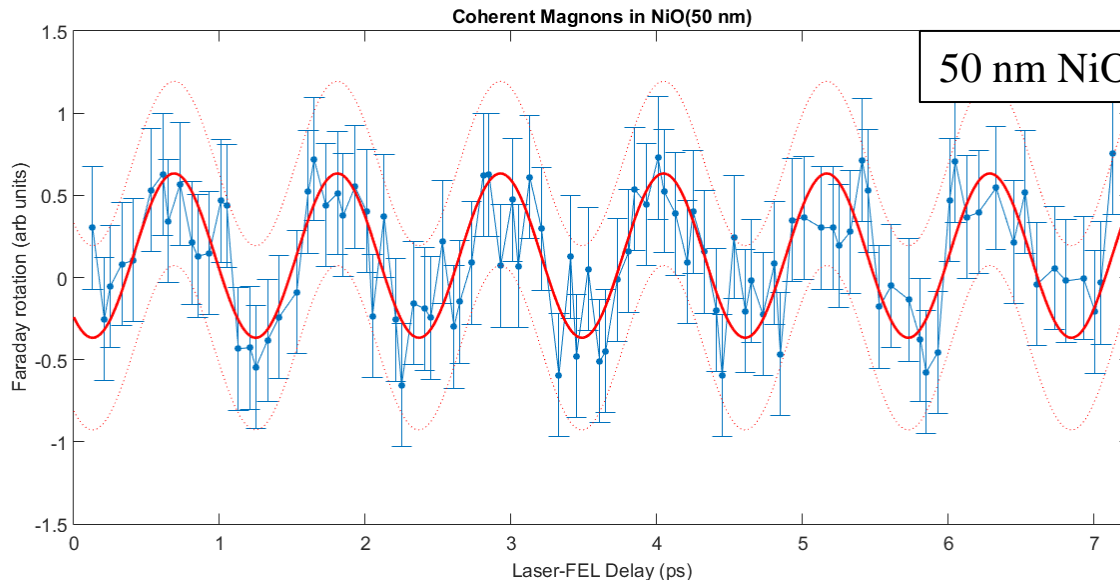


Elettra Sincrotrone Trieste

Optical TG used for probing **magneto-elastic waves** in Ni



one-to-one correspondence between **acoustic** and **magnetic** response



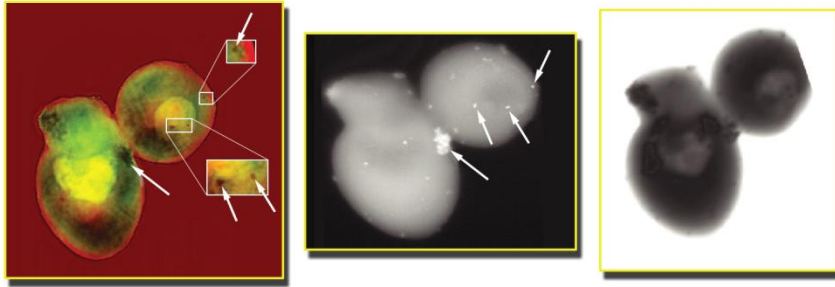
50 nm NiO on a **glass substrate**

Circ. Pol. FEL pulses on the Ni M edge generate single-mode coherent **magnon** in a prototypical AF insulator

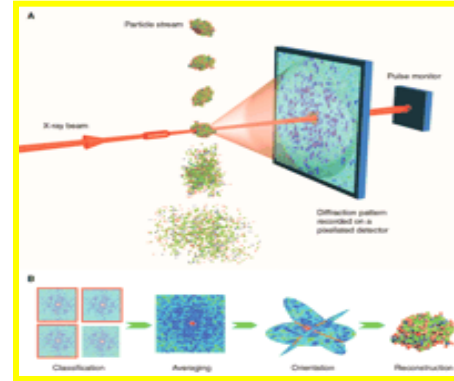
A. Simoncig et al., PRM 2017

Other applications

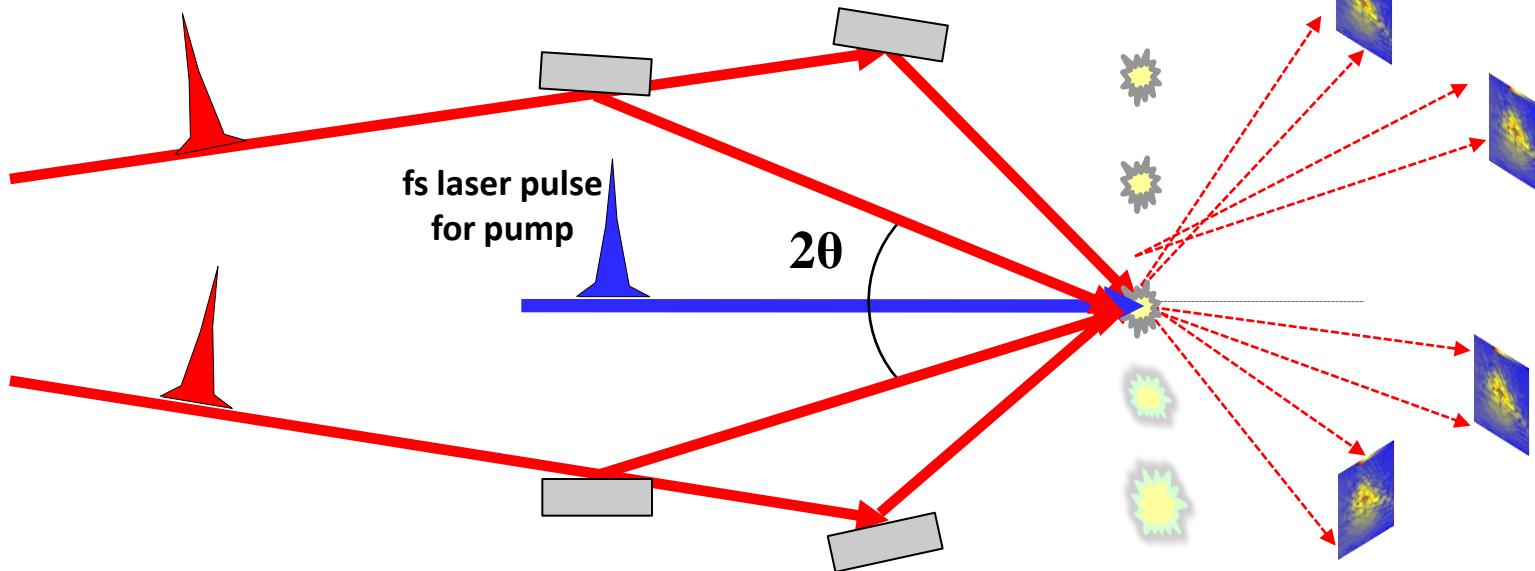
Example: **stereo** coherent diffraction imaging



Example: J. Nelson et al, PNAS 16 2010
The relationship of cell's internal structures can only be determined accurately by full 3-D imaging



FEL: 3D CDI-for random orientation delivery: via classification (Hajdu, Chapman)



Heat Transport, **Diffusion** Phenomena, Flow Studies, Concentration Grating,
Electronic **Energy Transfer**, Photochemical Reactions, Optical Damage

H. J. Eichler et al., J. Appl. Phys. 44, 5455 (1973)

REPORTS

30 MAY 2003 VOL 300 SCIENCE www.sciencemag.org

Diffusion of Nonequilibrium Quasi-Particles in a Cuprate Superconductor

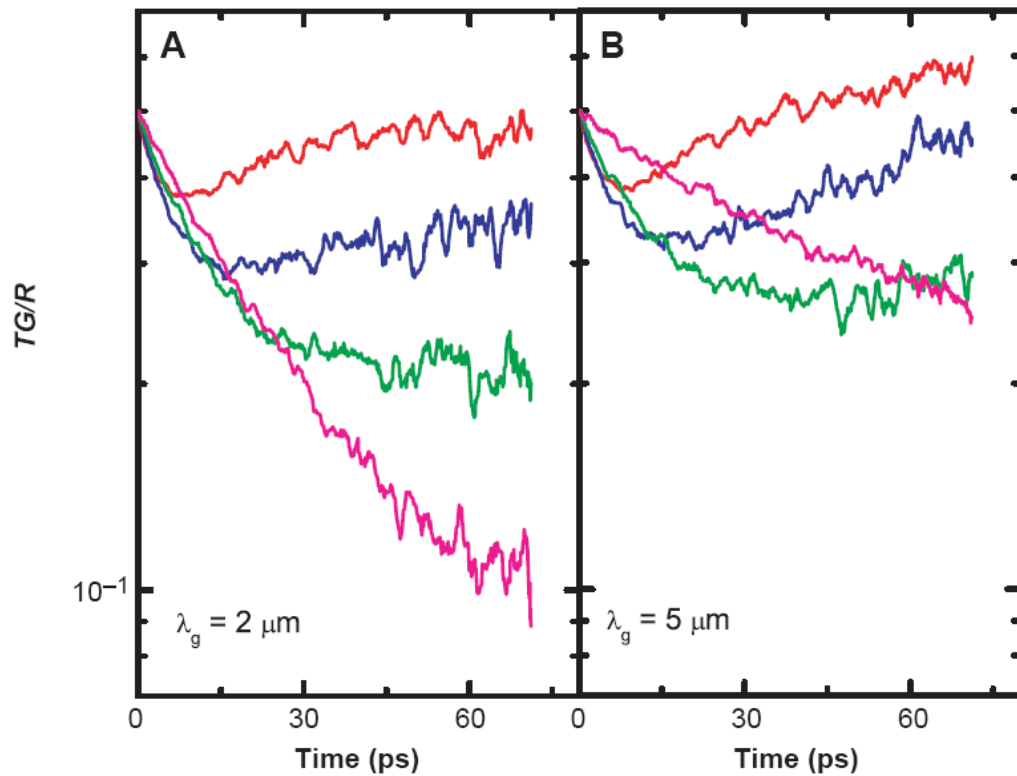
N. Gedik,¹ J. Orenstein,^{1*} Ruixing Liang,² D. A. Bonn,²
W. N. Hardy²

We report a transport study of nonequilibrium quasi-particles in a high-transition-temperature cuprate superconductor using the transient grating technique. Low-intensity laser excitation (at a photon energy of 1.5 electron volts) was used to introduce a spatially periodic density of quasi-particles into a high-quality untwinned single crystal of $\text{YBa}_2\text{Cu}_3\text{O}_{6.5}$. Probing the evolution of the initial density through space and time yielded the quasi-particle diffusion coefficient and the inelastic and elastic scattering rates. The technique reported here is potentially applicable to precision measurements of quasi-particle dynamics not only in cuprate superconductors but in other electronic systems as well.

Diffusion of Quasiparticles



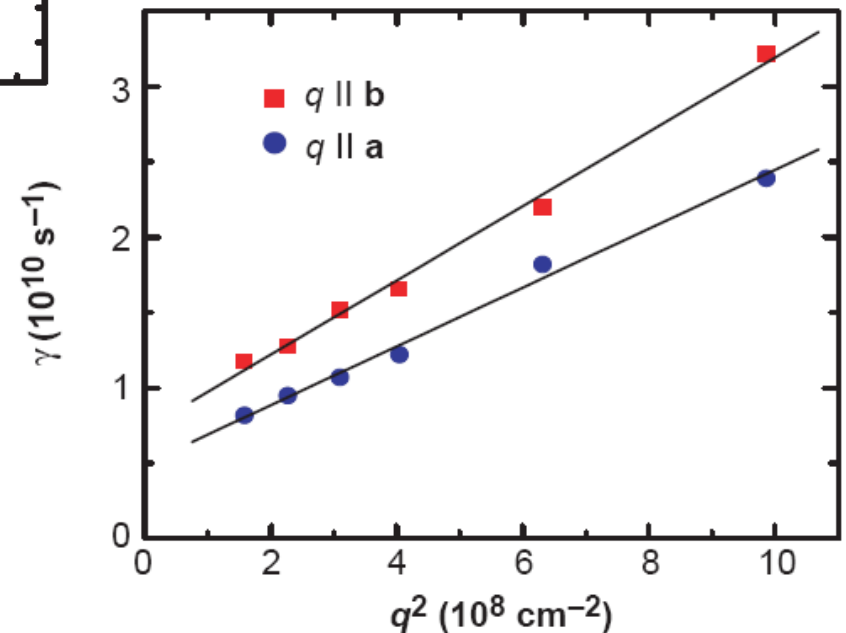
Elettra Sincrotrone Trieste



TG = Diffraction Efficiency
R = Specular Reflection

Diffusion of Quasiparticles is interesting for

- SC X-ray **Detectors**
- manipulation of SC based **Qubits**
- mechanism of Cooper pair in **HTSC**



TG can excite **Spin Waves** using orthogonal polarization

Letter

Nature **437**, 1330-1333 (27 October 2005) | doi:10.1038/nature04206; Received 29 April 2005; Accepted 2 September 2005

Observation of spin Coulomb drag in a two-dimensional electron gas

Spin Diffusion and Relaxation in a 2-dim. Electron Gas

C. P. Weber¹, N. Gedik^{1,2}, J. E. Moore¹, J. Orenstein¹, J. Stephens³ and D. D. Awschalom³

nature
physics

ARTICLES

PUBLISHED ONLINE: 11 DECEMBER 2011 | DOI: 10.1038/NPHYS2157

Doppler velocimetry of spin propagation in a two-dimensional electron gas

Luyi Yang^{1,2}, J. D. Koralek², J. Orenstein^{1,2*}, D. R. Tibbetts³, J. L. Reno³ and M. P. Lilly³

An electron propagating through a solid carries spin angular momentum in addition to its mass and charge. Of late there has been considerable interest in developing electronic devices based on the transport of spin that offer potential advantages in dissipation, size and speed over charge-based devices¹. However, these advantages bring with them additional complexity. Because each electron carries a single, fixed value ($-e$) of charge, the electrical current carried by a gas of electrons is simply proportional to its total momentum. A fundamental consequence is that the charge current is not affected by interactions that conserve total momentum, notably collisions among the electrons themselves². In contrast, the electron's spin along a given spatial direction can take on two values, $\pm\hbar/2$ (conventionally \uparrow, \downarrow), so that the spin current and momentum need not be proportional. Although the transport of spin polarization is not protected by

momentum conservation, it has been widely assumed that, like the charge current, spin current is unaffected by electron–electron ($e-e$) interactions. Here we demonstrate experimentally not only that this assumption is invalid, but also that over a broad range of temperature and electron density, the flow of spin polarization in a two-dimensional gas of electrons is controlled by the rate of $e-e$ collisions.

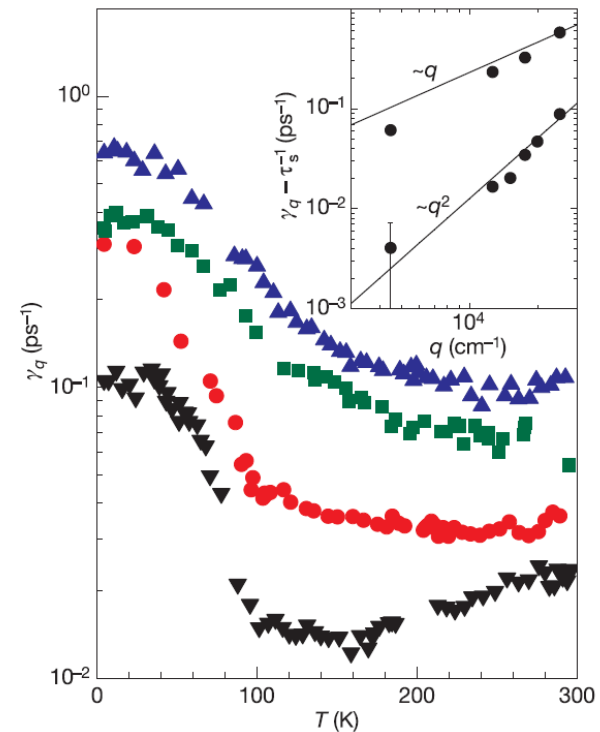


Figure 1 | Spin-grating decay at various wavevectors (q) and temperatures (T) for the sample with Fermi temperature 400 K. Main panel, the initial decay rate, γ_q , of the spin grating as a function of T for (bottom to top) $q = 0.45 \times 10^{-4}$, 1.3×10^{-4} , 1.8×10^{-4} and $2.5 \times 10^{-4} \text{ cm}^{-1}$. Inset, the initial decay rate of the spin grating as a function of q . Points are $\gamma_q - \tau_s^{-1}$; τ_s is obtained from decay of homogenous ($q = 0$) spin excitation. Error bars (s.d.) are the size of the points except as shown. Lower points and line, room temperature. The line is a fit of the data to $\gamma_q = \tau_s^{-1} + D_s q^2$, giving a spin diffusion length $L_s = (D_s \tau_s)^{1/2} = 0.81 \mu\text{m}$ and a ‘spin mean-free-path’ $l = 2D_s/v_F = 60 \text{ nm}$. The observation of diffusive motion is internally consistent, as l is much smaller than both L_s and the smallest grating wavelength, $2.5 \mu\text{m}$. Upper points and line, 5 K. The line has slope = 1, corresponding to ballistic, rather than diffusive, spin-motion with a velocity of $2.3 \times 10^7 \text{ cm s}^{-1}$.

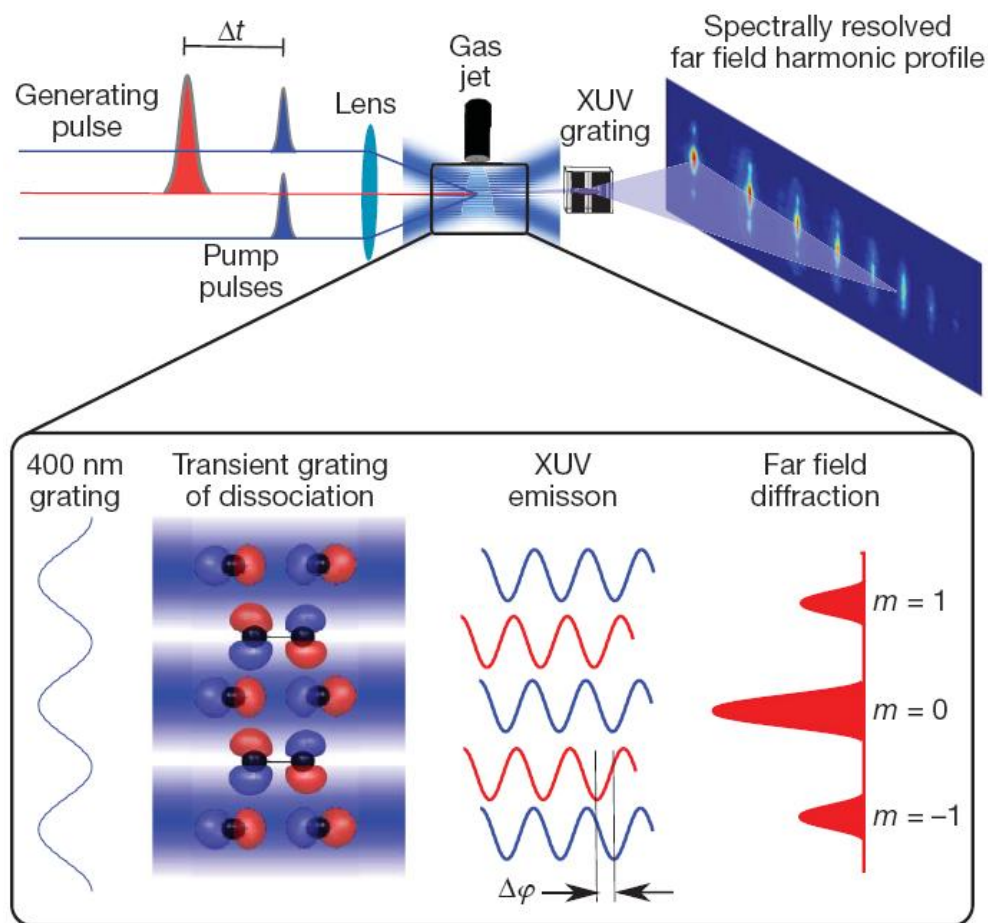
LETTERS

Following a chemical reaction using high-harmonic interferometry

H. J. Wörner¹, J. B. Bertrand¹, D. V. Kartashov^{1,2}, P. B. Corkum¹ & D. M. Villeneuve¹

The study of chemical reactions on the molecular (femtosecond) timescale typically uses pump laser pulses to excite molecules and subsequent probe pulses to interrogate them. The ultrashort pump pulse can excite only a small fraction of molecules, and the probe wavelength must be carefully chosen to discriminate between excited and unexcited molecules. The past decade has seen the emergence of new methods that are also aimed at imaging chemical reactions as they occur, based on X-ray diffraction¹, electron diffraction² or laser-induced recollision^{3,4}—with spectral selection not available for any of these new methods. Here we show that in the case of high-harmonic spectroscopy based on recollision, this apparent limitation becomes a major advantage owing to the coherent nature of the attosecond high-harmonic pulse generation. The coherence allows the unexcited molecules to act as local oscillators against which the dynamics are observed, so a transient grating technique^{5,6} can be used to reconstruct the amplitude and phase of emission from the excited molecules. We then extract structural information from the amplitude, which encodes the internuclear separation, by quantum interference at short times and by scattering of the recollision electron at longer times. The phase records the attosecond dynamics of the electrons, giving access to the evolving ionization potentials and the electronic structure of the transient molecule. In our experiment, we are able to document a temporal shift of the high-harmonic field of less than an attosecond ($1\text{ as} = 10^{-18}\text{ s}$) between the stretched and compressed geometry of weakly vibrationally excited Br_2 in the electronic ground state.

The ability to probe structural and electronic features, combined with high time resolution, make high-harmonic spectroscopy ideally suited to measuring coupled electronic and nuclear dynamics occurring in photochemical reactions and to characterizing the electronic structure of transition states.



Acknowledgments



L. Giannessi



M. Danailov



M. Zangrando



M. Kiskinova



F. Parmigiani



M. Svandrlík



F. Bencivenga



F. Cilento



F. Capotondi



M. Di Fraia



E. Principi



C. Callegari



O. Plekan



A. Gessini



D. Naumenko



E. Pedersoli



A. Perucchi



M. Malvestuto



M. Coreno



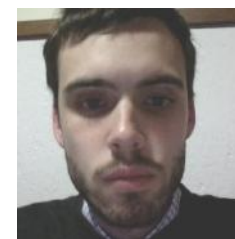
A. Simoncig



G. De Ninno



K. Prince



R. Mincigrucci



L. Foglia